High resolution X-ray detector for Astronomy and Astrophysics

Akhil Bhardwaj

Reg No: MS13041

A dissertation submitted for the partial fulfilment
of BS-MS dual degree in Science

Under the guidence of

Dr. Satyajit Jena

April 2018

Indian Institute of Science Education and Research Mohali

Sector - 81, SAS Nagar, Mohali 140306, Punjab, India

Certificate of Examination

This is to certify that the dissertation titled **"High resolution X-ray detector for Astronomy and Astrophysics"** submitted by **Akhil Bhardwaj** (Reg. No. MS13041) for the partial fulfillment of BS-MS dual degree programme of the Institute, has been examined by the thesis committee duly appointed by the Institute. The committee finds the work done by the candidate satisfactory and recommends that the report be accepted.

Prof. K.P. Singh Prof. R.S. Johal Dr. Satyajit Jena
(Supervisor)

Dated: 20.04.2018

Declaration

The work presented in this dissertation has been carried out by me under the guidance of Dr. Satyajit Jena at the Indian Institute of Science Education and Research Mohali.

This work has not been submitted in part or in full for a degree, a diploma, or a fellowship to any other university or institute. Whenever contributions of others are involved, every effort is made to indicate this clearly, with due acknowledgement of collaborative research and discussions. This thesis is a bonafide record of original work done by me and all sources listed within have been detailed in the bibliography.

Akhil Bhardwaj
(Candidate)

Dated: April 20, 2018

In my capacity as the supervisor of the candidate's project work, I certify that the above statements by the candidate are true to the best of my knowledge.

Dr. Satyajit Jena
(Supervisor)

Acknowledgment

I would first like to thank my thesis advisor Dr. Satyajit Jena at IISER Mohali. He was always there to support and help in any trouble I faced. He has constantly inspired me and motivated me, with his support and vision.

I thank Inspire-DST SHE for supporting me financially in the years of my masters degree. I thank IISER Mohali for providing me the facilities for the successful completion of my thesis work.

I would also like to thank the PhD seniors who were involved in the validation survey for this research project: Rohit Gupta, Nishat Fiza and Karthik. Without their passionate participation and input, the validation survey could not have been successfully conducted.

I also thank my lab mates Shubham Verma, Shahina, Tasha Gautam, Anjaly Menon for their constant support and help.

Finally, I must express my very profound gratitude to my parents, my sister and my friends Kalik Vashisth (aka kinkyG), Neeraj Maan (aka maan sahb), Prakhar Gahlot (aka Dg), Siddharth Kumar (aka Lappu), Asish Moharana (aka Princess) for providing me with unfailing support and continuous encouragement throughout my years of study and through the process of researching and writing this thesis. This accomplishment would not have been possible without them. Thank you.

Akhil Bhardwaj

Abstract

The emission of energy through a medium or space in the form of waves or particles is called radiation. Radiation can be an EM radiation, particle radiation, acoustic radiation or gravitational radiation.Dictated by the energy of the radiated particles, characterizing radiation as either ionizing or non-ionizing. The ionizing radiation which has energy more than 10 eV is able to ionize atoms or molecules and can break chemical bonds. The ionizing part of the Electromagnetic spectrum consists of Gamma rays, X-Rays, and the high energy UV light.

The radiation not only carries energy but also carries information about its source, which is useful to probe areas which are otherwise inaccessible. The source and how the source produces radiation decides the modulation of information. So, the study of radiation from a source can give us a significant amount of information about the source like its structure, chemical composition, matter configuration and a lot more. In observational astronomy studies distant objects by making observations in different parts of the EM spectrum, like optical astronomy, radio astronomy, X-Ray astronomy. For making such observations, we need better and more sophisticated eyes. Radiation detectors, help us to do so.

Here in this work focuses on new class of detectors for X-Ray astronomy, by dealing with some limitations of the current methods. As X-Rays are incapable of penetrating the earth's atmosphere, we need high altitude or space-based observatories, posing a different challenge. Using cost-effective Gaseous Ionization detectors can be a possible way forward. The use of Micro-pattern gas detectors can be possible way forward [BBB$^+$03], with the help of computer simulations can help to test these detectors for use in X-ray astronomy and astrophysics.

Contents

List of Figures

List of Tables

Chapter 1

X-ray Astronomy

1.1 Astronomical sources of X-rays

Astrophysical sources of X-rays - Several types of astrophysical objects emit, fluoresce, or reflect X-rays as [wikb]:-

1. Galaxy clusters, black holes in active galactic nuclei (AGN) to galactic objects such as supernova remnants, stars, and binary stars containing a white dwarf, neutron star or black hole (X-ray binaries).

2. Moon, though most of the X-ray brightness of the Moon arises from reflected solar X-rays.

3. A combination of many unresolved X-ray sources is thought to produce the observed X-ray background.

4. A combination of many unresolved X-ray sources is thought to produce the observed X-ray background.

5. The X-ray continuum can arise from bremsstrahlung, black-body radiation, synchronton radiation.

6. Galaxies or black holes at the centers of galaxies

7. Pulsars

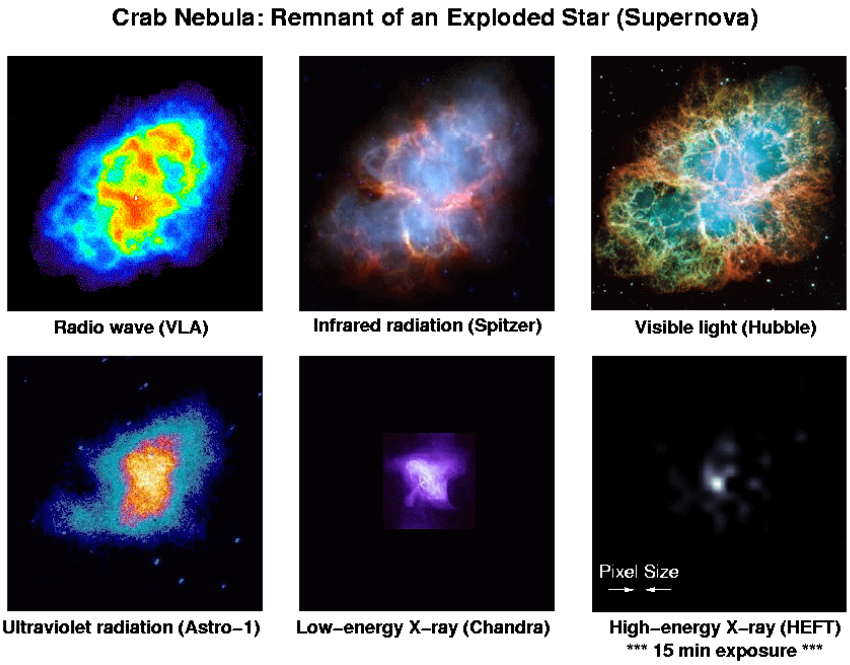

Figure 1.1: Crab Nebula in different wavelengths of EM spectrum [wikb]

1.2 X-ray astronomy

X-ray astronomy is an observational branch of astronomy which deals with the study of X-ray observation and detection from astronomical objects. X-ray emission is expected from astronomical objects that contain extremely hot gases at temperatures from about a million kelvin (K) to hundreds of millions of Kelvin (MK). X-radiation is absorbed by the Earth's atmosphere, so instruments to detect X-rays must be taken to high altitude or even outer space. X-ray astronomy can see farther than standard light-absorption telescopes, such as the Mauna Kea Observatories, via x-ray radiation. The total amount of hot gas is five to ten times the total mass in the visible. Many thousands of X-ray sources are known.

The X-rays have been observed enmantling from Sun since 1940, but in 1962 the discovery of the first cosmic X-rays source in the constellation Scorpius was the Scorpius X-1. The X-ray emission of Sco X-1 is 10,000 times greater than its visual emission, whereas that of the Sun is about a million times less. Sources as Sco X-1 are now identified as compact stars, such as neutron stars or black holes. Material falling into a black hole may emit X-rays, but the black hole itself does not. In falling gas and dust is heated by the strong gravitational fields of these and other celestial objects, gravity serves as energy source for X-Rays. Riccardo Giacconi received the Nobel Prize in Physics in 2002, for discoveries in

this new field of X-ray astronomy, starting with Sco X-1. [wikb]

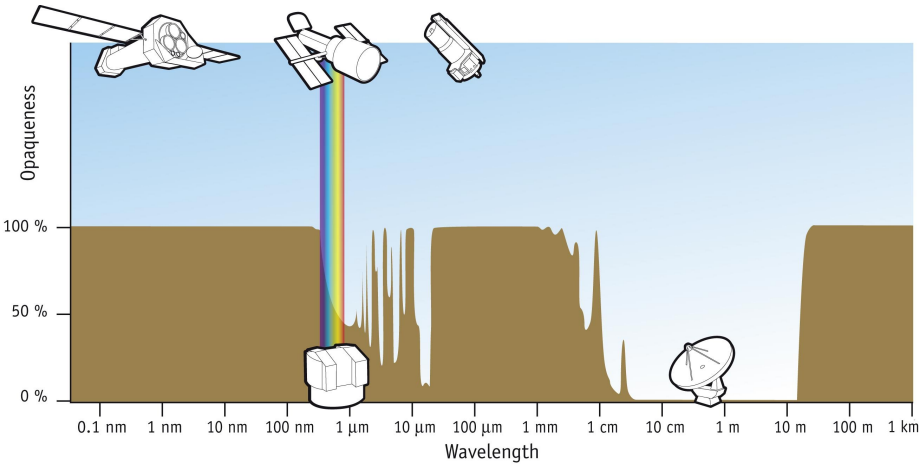

Figure 1.2: The opacity of the atmosphere to different wavelengths of EM radiation, it is opaque to X-rays from astronomical sources.

1.3 X-ray astronomy detectors

X-ray astronomy detectors have been designed and configured primarily for energy and occasionally for wavelength detection using a variety of techniques usually limited to the technology of the time.

X-ray detectors -

1. Collect individual X-rays (photons of X-ray electromagnetic radiation)
2. Count the number of photons collected (intensity)
3. The energy (ranging between 0.12 to 120 keV) of the photons collected
4. Wavelength of the X-rays detected (0.008 to 8 nm)
5. How fast the photons are detected (counts per hour), to tell us about the object that is emitting them.

1.4 Micropattern Gas detectors in X-ray astronomy

Micro pattern gas detectors are the gaseous ionization detectors developed for better spatial resolution and response time as a very small interaction volume is used, as compared

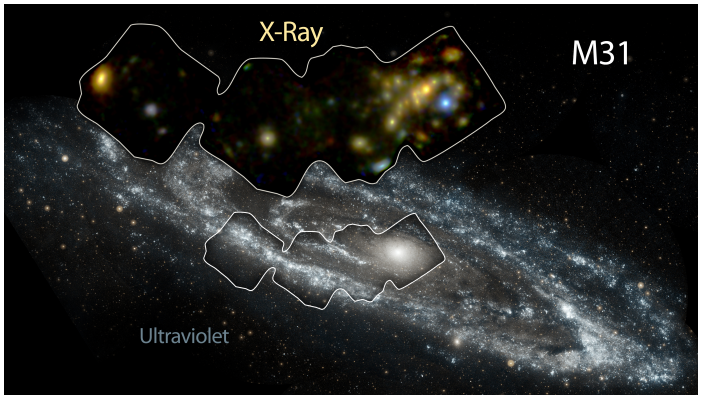

Figure 1.3: Andromeda Galaxy [goo]

to other gaseous ionization detectors. These detectors are basically charge amplifiers and can be used to amplify the amount of charge obtained form the interaction of radiation and matter. Gasses and gas mixtures of noble gases, noble gasses mixed with gasses like $Co_2, methane, SF_6$, are used as the medium that interacts with the radiation.

The applied potential inside the detector results in the high electric field, which makes the electrons produced in the ionization of the gas by the radiation, accelerate to such high energy that they start to ionize the surrounding gas atoms and molecules. Thus it forms an avalanche and the charge is amplified. Collecting this charge at the read-out strips results in the signal generation. The signal generated then can be analyzed using further electronics to extract information about the radiation itself.

The amount of charge collected is proportional to the energy of the incoming radiation hence obtaining information about the energy of the radiation is achievable.

Micropattern gas detectors have some useful features as listed below :[BBB$^+$06]

1. Cost effective
2. Gain constant over a wide temperature range.
3. Minimum perturbation on the impinging particles.
4. High gain typically $10^3 \ - \ 10^4$
5. High resolutions (typically $\sim 50\mu m$).
6. Very fast read out (in 100 ns)

7. Rate capability few MHz/mm^2 .

8. Can cover wide X-Ray band on proper optimization (100eV to 100keV and more)

9. Can do things like Polarization study [BAB+02]

As the X-ray radiation [wika] is ionizing radiation, thus these detectors can be used in X-ray detection and imaging after a proper optimization. Further, the detector can be optimized in such a way that it can provide information about different properties like polarization, energy spectrum, etc. of the radiation itself. The study of these properties can provide us with the information about the radiation source itself, which is important in X-ray astronomy.
One good area they can be useful is the area of X-ray polarimetry, where the track of the outgoing photoelectron can be recorded precisely and thus we can get the polarization of the X-ray coming from the distant source.
The work presented here looks into the possibility of using these detectors in X-ray astronomy. Using computer simulations for characterizing the detector for X-ray astronomy, testing the prospects of this proposal is easier as compared to making a prototype. These computer simulations help to understand the system in a better way before investing in a prototype.

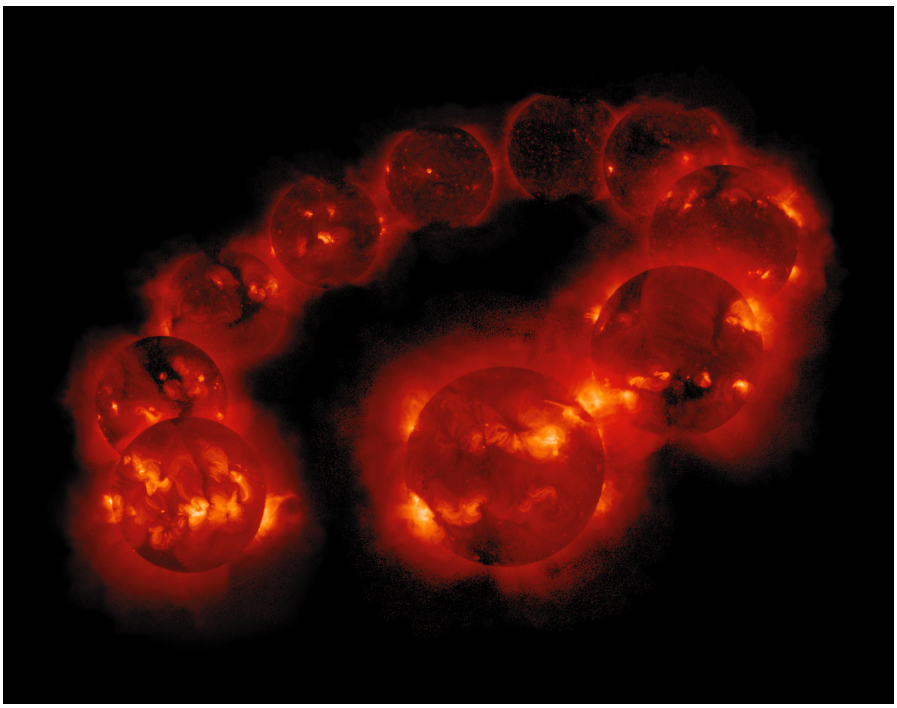

Figure 1.4: The Solar cycle in X-Ray [goo]

The next chapter discusses the interaction of radiation with matter, which is the main phenomenon in radiation detectors used for radiation detection.

Chapter 2

Radiation and matter

2.1 Radiation

The emission of energy through a medium or space in the form of waves or particles is called radiation. Radiation can be characterized as [rad]:

1. EM radiation:- Radio waves, microwaves, X-Rays
2. Acoustic radiation:- ultrasound, seismic waves.
3. Gravitational radiation:- Ripples in the curvature of space time.
4. Particle radiation:- α radiation, β radiation, neutron radiation.

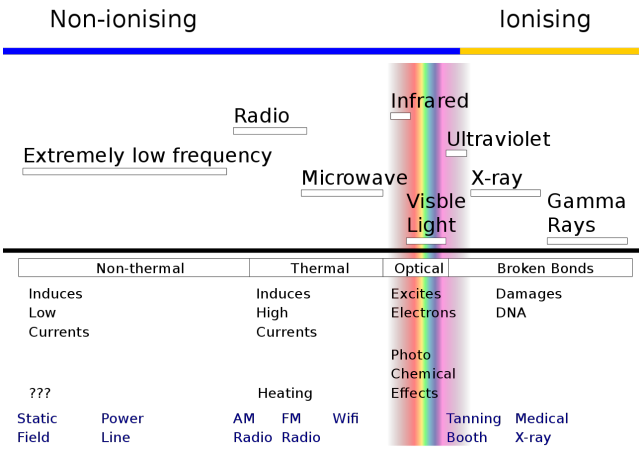

Figure 2.1: The EM spectra [goo]

The knowledge of the interactions which occur when radiation encounters matter and the interactions produce some effects. These processes are exploited by the particle detectors to gather information about the radiation itself. The radiation penetrating matter sees the matter in form of its basic constituents, i.e., as an aggregate of electrons and nucleons.
Different types of radiation depending on their energy and the also depending of the type of material they are interacting with, have reactions with the atom as a whole or the nuclei with its constituents. So, it depends on these factors that which process(es) will indeed happen. For example an alpha particle can just collide with an atomic electron or it can be absorbed by the atomic nucleus to undergo different nuclear reactions or just can bounce off the nuclei via Coulomb force. Considering the strength and long range of the Coulomb force, eletromagnetic processes are dominant processes most of the time.
In case of a neutral particle like neutron, the neutron can interact eletromagnetically (through its magnetic moment) and can also undergo processes involving weak interaction. It is dictated by the energy of the radiated particles, characterizing radiation as either ionizing or non-ionizing. The ionizing radiation which has energy more than 10 eV is able to ionize atoms or molecules and can break chemical bonds. The ionizing part of the Electromagnetic spectrum consists of Gamma rays, X-Rays and the high energy UV light.[Leo87]

2.2 The interaction of radiation with matter

2.2.1 The Cross Section

The Cross Section generally describes the collision or interaction of two particles. Consider one particle as the incident particle and other particle to be a fixed target. The incoming particles can be in form of a beam uniformly distributed in space and time with a defined *flux* of F number of particles incident per unit area per unit time. This tends towards $dN_s/d\Omega$, where N_s is the average number of particles scattered per unit time. The differential cross section is defined as

$$\frac{d\sigma}{d\Omega}(E,\Omega) \;=\; \frac{1}{F}\frac{dN_s}{d\Omega} \tag{2.1}$$

which implies that this ratio $\frac{d\sigma}{d\Omega}$ is the average fraction of the particles scattered into $d\Omega$ per unit time per unit flux (F). For quantum mechanical particles this ratio can be interpreted as the scattered probability current in the angle $d\Omega$ by the total incident probability passing

through a unit area in front of the target.The total cross section is the integral of equation (2.1) over all solid angles, i.e.,

$$\sigma(E) \;=\; \int d\Omega \frac{d\sigma}{d\Omega} \tag{2.2}$$

The average number of particles scattered into all angles is

$$N_s(\Omega) \;=\; FAN\delta x \frac{d\sigma}{d\Omega} \tag{2.3}$$

and the total number of particles scattered is

$$N_{tot} \;=\; FAN\delta x\sigma \tag{2.4}$$

where $N\delta x$ is the number of centers per unit perpendicular area which will be seen by the beam, FA gives the number of incident particles which are eligible for an interaction, A being the total perpendicular area of the target.

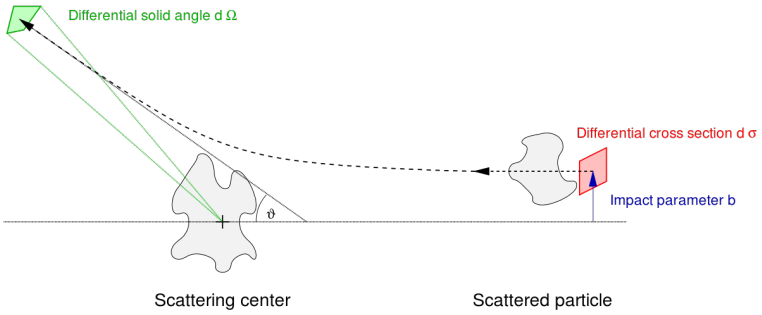

Figure 2.2: Differntial Cross Section schemetic

2.2.2 Mean Free Path

Mean free path is related to the probability for an interaction in a distance x. This is related to the problem of random walk, here the question is what is the probability that a particle will not suffer an interaction in a distance x ? which is also the survival probability. Let
$P(x) \;:\; Probability\ of\ not\ having\ an\ interaction\ after\ a\ distance\ x$
$w\ dx \;:\; Probability\ of\ having\ an\ interaction\ between\ x\ and\ x\ +\ dx$ The probability of not having an interaction between x and x+dx is

$$\begin{aligned} P(x+dx) \;&=\; P(x)(1-wdx) \\ P(x) \;+\; \frac{dP}{dx} \;&=\; P - Pwdx \\ \Longrightarrow\; P \;&=\; C\ exp(-wx) \end{aligned}$$

with C being a constant and the condition that $P(0) = 1 \implies C = 1$, thus the probability of survival is exponential in distance. The mean distance or the mean free path λ is given as

$$\lambda = \frac{\int xP(x)dx}{P(x)dx} = \frac{1}{w} \tag{2.5}$$

$$\lambda = \frac{1}{N\sigma} \tag{2.6}$$

$$\implies P(x) = exp\Big(\frac{-x}{\lambda}\Big) = exp(-N\sigma x) \tag{2.7}$$

$$P_{int}(x) = 1 - P(x) \tag{2.8}$$

where $P(x)$ is the survival probability and $P_{int}(x)$ is the probability of interaction.

2.3 Energy loss in matter

2.3.1 Energy Loss of Heavy Charged Particles

The passage of charged particles through matter is characterized by two principal features:

1. energy loss by the particle
2. deflection of the particle from its incident direction

These are due to the following processes:

1. Inelastic collisions with the atomic electrons of the material
2. Elastic scattering from nuclei
3. Cherenkov radiation
4. Nuclear reactions
5. Bremsstrahlung

The charged particles can be separated into following classes:

1. light particles : electrons and positrons
2. heavy particles : particles heavier than electrons, such as muons, α -particles
3. heavy ions : heavier than the second class

The charged particles interact with the matter prominently via eletromagnetic processes. The energy loss by heavy particles in matter is mainly due to the inelastic collisions based on Coulomb force.The atomic collisions of the charged particles can be hard collisions or soft collisions, where in the former case the atom is ionized, whereas in the later case the electron produced in the ionization has such a high energy (such an electron is called a delta electron or a δ -ray) that it produces further ionization.

In the case of elastic scattering very little energy is given in transfer due to the fact that the mass of the incoming particle is small compared to the mass of nuclei.

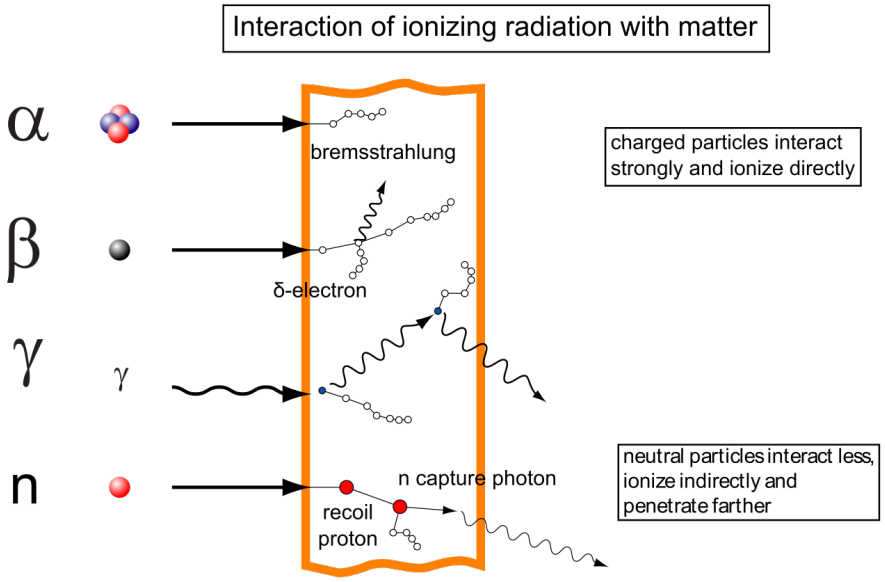

Figure 2.3: Interaction of matter and Ionizing radiation

2.3.2 The Bethe-Bloch formula

The inelastic collisions are statistical in nature, thus the average energy loss per unit path length is relevant. This quantity is called as the stopping power or simply dE/dx.

The Bethe-Bloch formula takes into account the quantum-mechanical treatment of the collision process. The formula is given as

$$-\frac{dE}{dx} = 2\pi N_a r_e^2 m_e c^2 \rho \frac{Z}{A}\frac{z^2}{\beta^2}\left[ln\left(\frac{2m_e\gamma^2 v^2 W_{max}}{I^2}\right) - 2\beta^2\right] \tag{2.9}$$

with

$$2\pi N_a r_e^2 m_e c^2 = 0.1535\ MeV cm^2/g \tag{2.10}$$

$$
\begin{aligned}
e &: the\ charge\ of\ an\ electron \\
r_e &: classical\ electron\ radius\ =\ 2.817x10^{-13}cm \\
m_e &:\ Electron\ mass \\
N_a &: Avagadros's\ number = 6.023 \times 10^{23} per\ mol \\
I &: Mean\ excitation\ potential \\
Z &: atomic\ number\ of\ absorbing\ material \\
A &: atomic\ weight\ of\ absorbing\ material \\
\rho &: density\ of\ absorbing\ material \\
z &: charge\ of\ incident\ particles\ in\ units\ of\ e \\
\beta &: v/c\ of\ the\ incident\ particle \\
\gamma &: \frac{1}{\sqrt{1-\beta^2}} \\
W_{max} &: maximum\ energy\ transfer\ in\ a\ single\ collision
\end{aligned}
$$

The maximum energy transfer produced in head-on collision with a the mass of incident particle M is

$$W_{max} \ = \ \frac{2m_e c^2 \eta^2}{1 + 2s\sqrt{1+\eta^2+s^2}} \tag{2.11}$$

where $s \ = \ m_e/M$ and $\eta \ = \ \beta\gamma$, as $M \ \gg \ m_e$, so,

$$W_{max} \ = \ 2m_e c^2 \eta^2 \tag{2.12}$$

A simulation result for the stopping power of μ^+ in Cu is shown in Fig(2.4)

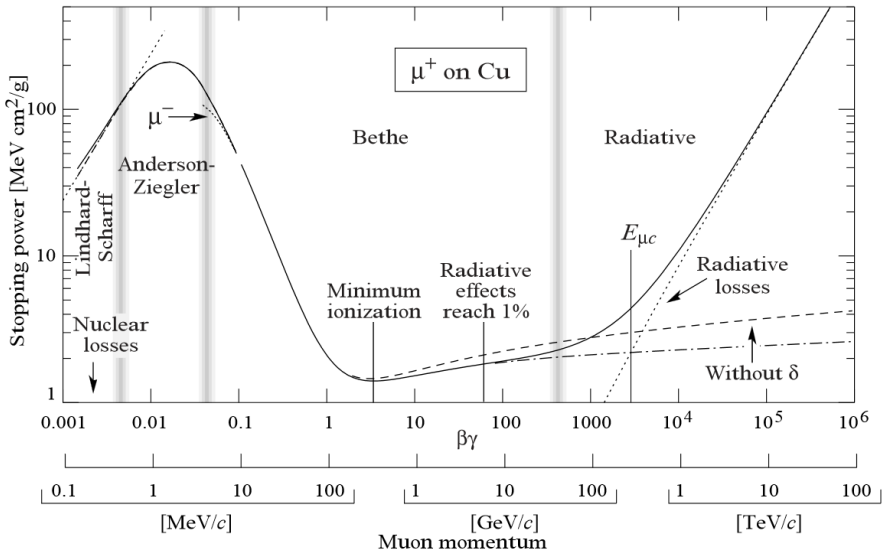

Figure 2.4: Bethe-Bloch formula simulation for μ^+ in copper [goo]

dE/dx for mixtures and compounds

For the case of mixtures and compounds a good estimate for the Bethe-Bloch formula can be found by averaging dE/dx over each element in the compound weighted by the fraction of electrons in each atom, this is called the *Bragg's rule*

$$\frac{1}{\rho}\frac{dE}{dx} = \sum_i \frac{w_i}{\rho_i}\left(\frac{dE}{dx}\right)_i \tag{2.13}$$

The specific terms are affected in the Bethe-Bloch Formula, they are

$$Z_{eff} = \Sigma a_i Z_i \tag{2.14}$$

$$A_{eff} = \Sigma a_i A_i \tag{2.15}$$

$$\ln I_{eff} = \sum_i \frac{a_i Z_i ln I_i}{Z_{eff}} \tag{2.16}$$

where a_i is the number of atoms if the i^{th} element and the index *i* is for the i^{th} element. The w_i is the fraction by weight of the i^{th} element

$$w_i = \frac{a_i A_i}{A_{eff}} \tag{2.17}$$

2.4 Photon energy loss in matter

2.4.1 Interaction of photons

As photons are charge less particles they interact with matter differently in comparison to charged particles. Due to the lack of charge, it is impossible to have elastic collisions with atomic electrons, which is a prominent feature in the interaction of charged particles.Photons ($X - rays\ and\ \gamma\ rays$) interact with matter in following three ways: Photoelectric effect, Compton scattering and Pair Production [individual discussion later in (2.4.2)].The two qualitative features of $X - rays\ and\ \gamma\ rays$ interaction that distinguish them from the interactions charged particles are:

1. the photons are way more penetrating in matter than charged particles

2. a beam of photons is not degraded in energy as it passes through matter, but is only reduced in intensity.

The first feature is explained by the fact that photons interactions have much smaller cross section relative to the inelastic interactions that charged particles undergo. The second feature is due to the fact that the photon is completely removed from the beam entirely in an interaction with matter, without affecting the other photons. Thus the other photons retain their original energy, however the total number of photons reduces. The attenuation suffered by a photon beam decreases exponentially with the absorbent thickness, i.e.,

$$I(x) \ = \ I_0 exp(-\mu x) \tag{2.18}$$

where I_0 : is the incident beam intensity; x : is the thickness of absorber; μ : is the absorption coefficient, μ is characteristic of the absorber medium.

2.4.2 Types of photon interactions

1. **Photoelectric effect**

   In Photoelectric (photon-electron interaction) effect, there is a transfer of all the energy of the photon to an electron which is located in one of the atomic shells. The photon energy is divided into two parts, one part is used to overcome the electron's binding energy and other provides kinetic energy to the electron. The electron looses

its energy rapidly and travels only a short distance from its original location. The energy of the out going electron is

$$E \;=\; h\nu \;+\; B.E. \tag{2.19}$$

where $B.E.$ is the binding energy of the electron. The cross section fro the processes in which the energy of the photon is just above a specific absorption edge (like K-absorption edge, L-absorption edge, M-absorption edge) is the maximum when the electron resides in the respective shell. The cross section for a photoelectric process can be calculated, though not in a rigorous way due to the complexity of Dirac wave-functions for atomic electrons. For non relativistic photon energy, i.e., $h\nu \ll m_e c^2$, using the Born approximation the cross section can be calculated as

$$\Phi_{photo} \;=\; 4\sqrt{2}\,\alpha^4 Z^5 \phi_0 \Big(\frac{m_e c^2}{h\nu}\Big)^{7/2} \tag{2.20}$$

with $\phi_0 \;=\; \frac{8\pi r_e^2}{3} \;=\; 6.651 \times 10^{-25}\; cm^2; \alpha \;=\; \frac{1}{137}$ In the whole process the photon energy is deposited by the photoeletron in the surrounding matter.

2. **Compton scattering**

In Compton Interaction only a part of the energy is absorbed and a photon is released with reduced energy.The direction of the leaving photon is different form the original photon, due to this change in direction this process is regarded as a scattering process. If the photon energy is high with respect to the B.E., the electrons can be considered essentially free. Following relations considering the energy and momentum conservation.

$$h\nu^{'} \;=\; \frac{h\nu}{1+\gamma(1-\cos\theta)} \tag{2.21}$$

$$T \;=\; h\nu - h\nu^{'} \;=\; h\nu \frac{\gamma(1-\cos\theta)}{1+\gamma(1-\cos\theta)} \tag{2.22}$$

$$\cos\theta \;=\; 1 - \frac{2}{(1+\gamma)^2 \tan^2\phi + 1} \tag{2.23}$$

$$\cot\phi \;=\; (1+\gamma)\tan\frac{\theta}{2} \tag{2.24}$$

The differential cross section for Compton scattering was calculated using QED and is called the *Klien-Nishina* formula

$$\frac{d\sigma}{d\Omega} \;=\; \frac{r_e^2}{2}\frac{1}{[1+\gamma(1-\cos\theta)]^2}\Big(1+\cos^2\theta + \frac{\gamma^2(1-\cos\theta)^2}{1+\gamma(1-\cos\theta)}\Big) \tag{2.25}$$

3. **Pair Production**

   For photon energies in excess of 1.022 MeV, the interaction of photon and matter can produce matter and anti-matter pairs, each part of the pair with equal mass. The photon interacts with the nucleus in such a way that it's energy is converted into matter. The process of pair production is theoretically related to bremsstrahlung. The nucleus plays an important role in the the process of pair production as in bremsstrahlung. It follows that the cross section for the pair production process is dependent on a parameter ξ which takes into account the effect of screening

$$\xi = \frac{100 m_e c^2 h\nu}{E_+ E_- Z^{1/3}} \tag{2.26}$$

   Where E_+ : total energy of the outgoing positron E_- : total energy of outgoing electron.

   Using the Born approximation following formula is obtained for extreme relativistic energies and arbitrary screening.

$$d\sigma = 4Z^2 r_e^2 \alpha \frac{dE_+}{(h\nu)^3} \Bigg[(E_+^2 + E_-^2)\Big(\frac{\phi_1(\xi)}{4} - \frac{1}{3} lnZ - f(Z)\Big) + \frac{2}{3} E_+ E_- \Big(\frac{\phi_2(\xi)}{4} - \frac{1}{3} lnZ - f(Z)\Big)\Bigg] \tag{2.27}$$

   here ϕ_1 and ϕ_2 are the screening functions

These are the processes and effects that occur when radiation interacts with the matter. The next chapter discusses about the class of radiation detectors called as the Gaseous Ionization detectors.

Chapter 3

Gaseous Ionization detectors

Gaseous Ionization Detectors use ionization effect of radiation on a gas-filled sensor.For a radiation to be detected it should have enough energy to ionize atoms or molecules of the gas medium.The ions and electrons thus produced cause a flow of current which is measured. [Leo87]

3.1 General principles

The passage of a charged particle or ionizing radiation excites and ionizes molecules along its path, thus producing a free electron-ion pair. Ion pairs thus produced are N_i in number

$$N_i = \frac{E_{abs}}{W} \tag{3.1}$$

where E_{abs} is the absolute energy of the incoming particle and W is the work function of the gas atom or molecule.

Then a collection mechanism is required otherwise the ion pairs loose energy and come to a thermal equilibrium and they recombine. The application of an electric field between two electrodes makes the charges, both +ve and -ve, drift and accelerate towards the electrodes along the field lines. The accelerating ion pairs are interrupted by collisions with the gas molecules, thus the average drift velocity of the charge in the direction of field backs to zero on a microscopic scale, but on a macroscopic level, there is a constant drift velocity along the direction of the electric field.

Thus a diffusion is superimposed on the drift velocity. This drifting charge results in the measured signal.The basic configuration consists of a container (can be of any shape as per

the requirements), with conducting walls and a thin end window. The container is filled with a suitable gas usually the nonreactive Nobel gases like argon. A thin metallic wire at a positive voltage $+V_0$, relative to the grounded wall is suspended in the middle of the chamber such that the wire is parallel to the chamber walls. The electric field inside such a chamber is

$$E = \frac{1}{r} \frac{V_0}{\ln(b/a)} \tag{3.2}$$

where r is the radial distance from the wire inside a the cylinder of radius a.

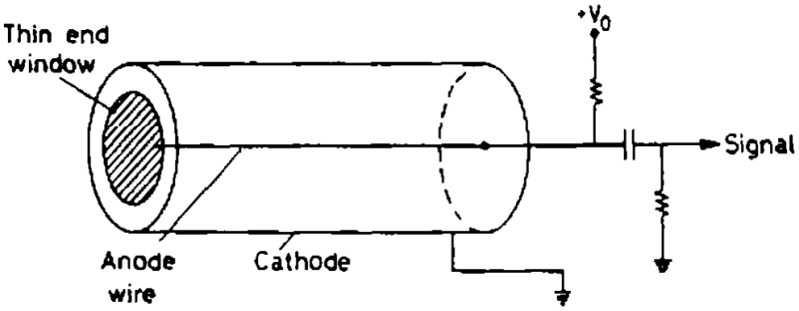

Figure 3.1: Basic schematic of a cylindrical Gaseous Ionization detector [Leo87]

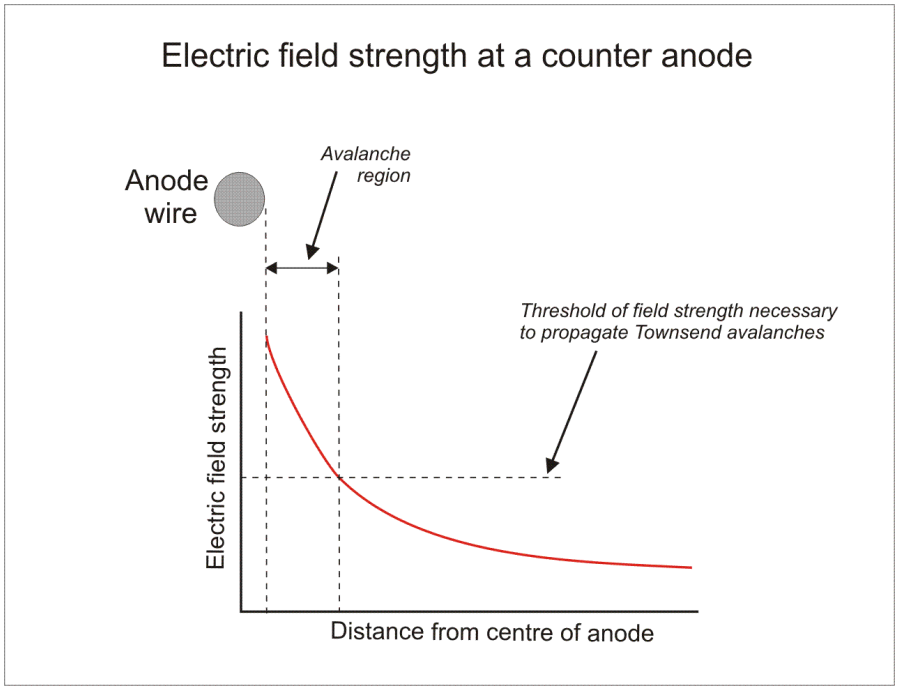

Figure 3.2: Electric field near the electrode [goo]

3.2 General Characteristics

For the detection of radiation, it is necessary that the detection medium used in the detector, interacts with the incoming radiation. This interaction is mainly a electromagnetic interaction in the case of charged particles. Even in the case of neutral particles there is need of a chemical or nuclear reaction. Most of the detectors we use nowadays are electrical in nature, and at some point transform the information contained by the radiation into electrical pulses or signals which can be treated to extract that information. So, electronics used for processing the signal impulse are important. Some detectors cannot be exploited unless we have sophisticated electronics in support.

3.2.1 Sensitivity

It is the capability of a detector to produce a usable signal for a given type of energy or radiation, thus a single detector cannot be sensitive to all types of radiation in given energy range. Outside that region the detector has decreased efficiency. The sensitivity of a detector depends on many factors:

1. The cross section for the interactions of the radiation with the detector medium.
   The probability of detection is basically dependent on the probability of interaction between the radiant particle and the detection medium.

2. The inherent noise in the detector
   The signal produced by the detector should be reasonably above the basic inherent noise in the detector for the signal to be usable and separated form the noise.

3. The mass of the detector
   Detection of particles like neutrinos is difficult as they hardly interact and this requires to increase the amount of detection medium so that we have a higher interaction probability.

4. The material used to protect and separate the sensitive medium inside the detector
   We need to protect the inside of the detector from damage, so, people use protective layers outside the detector. This may hinder the detector operation, thus a optimized solution is used.

3.2.2 Detector response

The detectors are also able to provide information about the energy of the radiation. The amount of ionization produced by the radiation inside the detector is proportional to the energy deposited by the radiation inside the detector. This information may or may not be preserved as the signal is processed.

The amount of charge deposited by the pulse provides the information about the amount of ionization, i.e., which can be obtained by integrating the pulse with respect to time. The integral is proportional to the amplitude or the height of the pulse. The relation between the total charge deposited or the pulse height of the signal out from the detector is the *response* of the detector. Ideally the response should be linear but is not the case always. Generally the response of the detector is a function of particle type and energy, thus a detector can respond linearly to one particle type but may not of other particles.

3.2.3 Energy Resolution: The Fano Factor

The energy resolution is an important factor when detectors are designed to measure the energy of the incident radiation. This shows the extent to which two close lying energies can be distinguished apart. Ideally the spectrum for a mono-energetic beam of radiation should be a delta-function peak but due to the fluctuations in the number of excitation and ionization produced, the observed spectrum is Gaussian in shape.

The resolution is measured in terms of *full width at half maximum* of the spectrum peak. Let ΔE be the width and E the energy, then the relative resolution is

$$Resolution \; = \; \frac{\Delta E}{E} \tag{3.3}$$

Equation (3.3) is expressed in percentage usually. Generally the resolution is related to the energy deposited in the detector, with the ratio improving with higher energy. The reason for that is the ionization and excitation follow Poission-like statistics. It is known that the energy required to produce an ionization is a constant, dependent on the material used, w. Therefore number of expected ionization events are $J = E/w$, therefore an increase in the incident energy, increases the number of ionization, but this also increases the fluctuations due to the ionization events.

The calculation of those fluctuations requires us to consider two cases. A detector in which the full energy of the radiation particle is not absorbed, the energy loss per unit length

is dE/dx, then the number of reactions that contribute in the signal production follow a Poisson distribution with variance

$$\sigma^2 = J \tag{3.4}$$

The energy dependence of the resolution is given as

$$R \;=\; 2.35\frac{\sqrt{J}}{J} \;=\; 2.35\sqrt{\frac{w}{E}} \tag{3.5}$$

where the factor 2.35 relates the standard deviation of the Gaussian distribution to its FWHM. Equation (3.5) shows that the resolution is inversely related to the square root of energy.

All the ionization events are not independent hence the resolution calculated using Poisson statistics is way higher than the actual value. $Fano$ calculated the variance under such a condition to be

$$\sigma^2 = FJ \tag{3.6}$$

where F is called the Fano factor. The Fano factor is a function of all the various processes that can lead to an energy transfer in the detector, and is dependent on the detector medium. Thus the resolution is given by

$$R \;=\; 2.35\frac{\sqrt{FJ}}{J} \;=\; 2.35\sqrt{\frac{Fw}{E}} \tag{3.7}$$

For $F = 1$ it is same as the case with a Poisson distribution.For detectors like semiconductor detectors or gas detectors $F < 1$, which implies the resolution increases a lot.

3.2.4 Detector Efficiency

A detector has two types of efficiency for radiation detection:

1. Absolute efficiency
2. Intrinsic efficiency

The efficiency of a detector is determined by the ratio of the number of events registered by the detector to the total number of events emitted by the source, i.e.,

$$\epsilon_{tot} \;=\; \frac{events\ registered}{events\ emitted\ by\ the\ source} \tag{3.8}$$

This is a function of the detector geometry and the interaction probability. For example for a cylindrical detector with a point source of radiation along its axis, the probability of a particle being emitted at an angle θ is

$$P(\theta)d\Omega = \frac{d\Omega}{4\pi} \tag{3.9}$$

Then the probability of a particle hitting the detector considering the geometry and the interaction probability is

$$d\xi_{tot} = \left[1 - exp\left(\frac{-x}{\lambda}\right)\right]\frac{d\Omega}{4\pi} \tag{3.10}$$

where x is the path length in the detector and λ is the mean free path for an interaction. Integrating (3.10) gives us the total efficiency.

The absolute efficiency has two parts:

1. Intrinsic efficiency ξ_{int}
2. Geometrical efficiency or acceptance ξ_{geom}

Then

$$\xi_{tot} = \xi_{int}\xi_{geom} \tag{3.11}$$

here the intrinsic efficiency is given by

$$\xi_{int} = \frac{events\ registered}{events\ impringing\ on\ the\ detector} \tag{3.12}$$

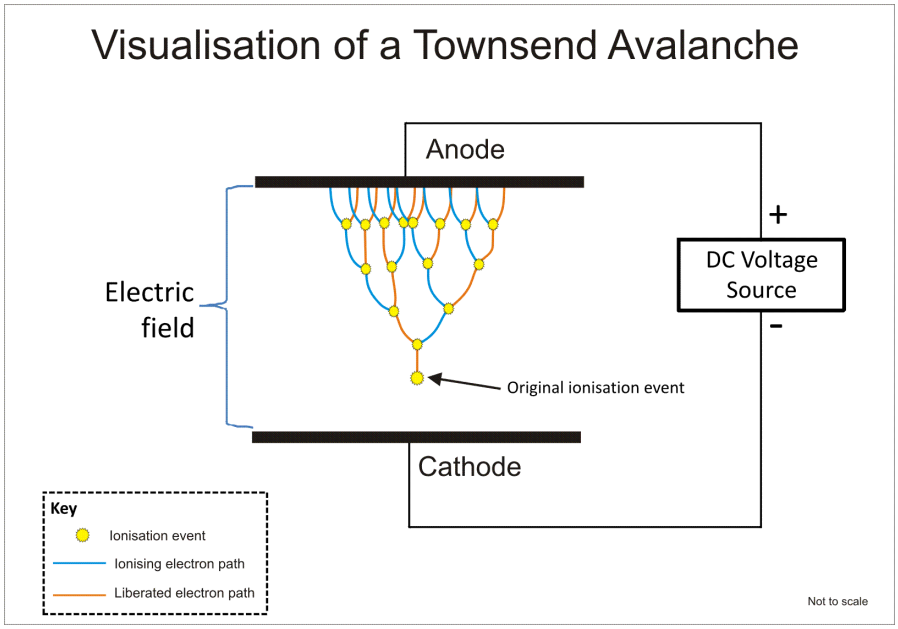

Figure 3.3: Visualization of a Townsend Avalanche [goo]

3.3 Properties of charge transport and ionization in gas

3.3.1 Ionization Mechanism

A charged particle can lose its energy in matter, essentially in two ways or two types of reaction.

1. Excitation

$$Y + p \longrightarrow Y^* + p \tag{3.13}$$

this is a resonant reaction (3.13), so requires the correct amount of energy transfer. These reactions have a typical cross-sections of the order of $\sigma = 10^{-17} cm^2$. While no electron -ion pairs are formed, but the excited atom or molecule can participate in further reactions that may lead to an ionization event.

2. Ionization

$$Y + p \longrightarrow Y^+ + p + e \tag{3.14}$$

This process has no exact energy requirement and has a higher cross-section with $\sigma = 10^{-16} cm^2$. Since the threshold requirement for a ionization process is relatively high as compared to the excitation processes, the later generally dominates. The creation of electrons and ions by the incident radiation is called as the primary ionization. A large amount of energy can be transferred to an electron such that this electron can produce further electron-ion pairs, this electron is called as the *delta electron* (delta ray).

A second mechanism of ionization of gasses called the *Penning Effect*. Certain atoms in their excited state do not immediately de-excite giving out a photon, but they may de-excite through a collision with another atom resulting in the ionization of the latter (3.15). For example noble gases.

$$Ne^* + Ar \longrightarrow Ne + Ar^+ + e^- \tag{3.15}$$

There is a third mechanism of ionization is the formation of molecular ions, this happens when a positive gas ion interacts with a neutral atom of the same type forms a molecular ion (3.16).

$$He^* + He \longrightarrow He_2^+ \tag{3.16}$$

3.3.2 Electron-ion pairs created

The occurrence of the ionizing reactions in a gas volume is statistical in nature, so identical particles do not in general, produce the same number of electron-ion pairs. Still we can have on an average estimate of the number of electron-ions created. This however is not equal to the energy loss divided by the ionization potential, as some energy is lost during excitation of the gas atoms and molecules. For gases the loss on an average is 1 pair per 30eV of energy lost.The efficiency and resolution (3.17) of the detector is determined by the average energy w required for creating an electron-ion pair. The resolution for a particle with energy E is

$$R \ = \ 2.35\sqrt{\frac{Fw}{E}} \tag{3.17}$$

where F is the Fano factor for the particular gas medium, which is not well determined but it should be less than 1.

3.3.3 Mean free path and Cross Section

The probability per unit time (τ^{-1}) to have a collision with another molecule or atom is

$$\tau^{-1} =< \nu_r > \sigma_0 N \tag{3.18}$$

assuming σ_0 to be constant cross section and $< \nu_r >$ the relative velocity of the two particles, given as

$$\vec{\nu_r} = \vec{\nu}_A + \vec{\nu}_B \tag{3.19}$$

$$\implies < \nu_r^2 > =< \nu_A^2 + \nu_B^2 - 2\vec{\nu}_A\vec{\nu}_B > \tag{3.20}$$

The arbitrary direction of the velocities makes the scalar product zero and

$$< v_r >= \sqrt{2} < v > \tag{3.21}$$

The mean free path or the mean distance covered between two collisions for a atom or molecule in the gas

$$\lambda =< \nu > \tau = \frac{1}{\sqrt{2}}\sigma_0 N \tag{3.22}$$

hence λ depends on the pressure of the gas i.e. the density via N. Here $\sigma_0 = \pi d^2$ for a molecule approximated as a sphere of radius d. Hence as the pressure decreases down the free path increases.

3.3.4 Diffusion

The neutral molecules and atoms is a gas are in a constant thermal motion, with velocities distributed according to the Maxwell-Boltzmann distribution function (3.23) $f(\vec{v})$

$$f(\vec{v})d\vec{v} = (\frac{m}{2\pi kT})^{3/2} \exp{(\frac{-mv^2}{2kT})}d\vec{v} \tag{3.23}$$

where k is the Boltzmann constant, T is the Temperature, m is the mass of the gas particle. Then the mean velocity (3.24) is:

$$< v >= \sqrt{\frac{8kT}{\pi m}} \tag{3.24}$$

For example the e^- have $< v_{e^-} >= 10^5 m/s$ and Ar ions have $< v_{Ar} >= 370 m/s$
In the absence to electric field the electrons and the ions interact with the molecules in the gas to give up their energy and go into a thermal equilibrium. For an initially localized charge distribution the diffusion due to collisions with the gas molecules follows a Gaussian distribution (3.25) as in 3D

$$dN\vec{r} = (\frac{N_0}{4\pi Dt})^{3/2} exp(-\frac{r^2}{4Dt})d\vec{r} \tag{3.25}$$

where D($m^2 s^{-1}$) is the diffusion constant which depends on the charge, the gas and the temperature. The form is reduced to a 1D form by replacing $\vec{r}$ with the linear variable x, with the characteristic variance $\sigma^2 = 2Dt$. In the presence of applied electric field the electrons and ions move to anode and cathode, respectively, with the thermal and drift motion superimposed. The electrons with small mass drift faster than ions with larger mass.

Transport of electrons

As electrons have a small mass their diffusion is in a quasi-isotropic way in all directions. Given that in an interaction an electron receives a velocity $\vec{v}_0$, then just before the next collision the velocity of the electron is

$$\vec{v} = \vec{v}_0 - \frac{eE}{m} eEt_c \tag{3.26}$$

which on average is

$$u =< v >= \frac{eE}{m}\tau \tag{3.27}$$

The energy provided by the electric field and the energy lost during collisions compete. For a drift distance x the e^- has $\frac{x}{u\tau}$ number of collisions, then the electron loses a fraction γ of the energy ϵ provided by the electric field. For energy balance we have

$$\frac{x}{u\tau}\gamma\epsilon = eEx \tag{3.28}$$

Considering the electrons have a larger instantaneous velocity than that of the gas atoms then

$$\epsilon = \frac{1}{2}mv^2 \; and \; \frac{1}{\tau} = N\sigma_0 v \tag{3.29}$$

using the above two equations we have

$$uv = \frac{eE}{mN\sigma_0} \; and \; \frac{1}{2}mv^2 = \frac{eEu}{N\sigma_0\gamma v} \tag{3.30}$$

$$\implies u^2 = \frac{eE}{mN\sigma_0}\sqrt{\frac{\gamma}{2}} \; and \; v^2 = \frac{eE}{mN\sigma_0}\sqrt{\frac{2}{\gamma}} \tag{3.31}$$

Hence the drift velocity depends on the value of E/N ratio of E/p, the reduced electric field for a fixed temperature.

Transport of ions

The ion (mass M_i) with each collision with a gas molecule (mass M_m) loses more and more energy in a non isotropic way, i.e. it partially remembers its trajectory before the collision.The drift vlocity can be calculated as

$$u = (\frac{1}{3M_{im}kT})^{\frac{1}{2}}\frac{eE}{N\sigma_0} \; for \; small \; E \tag{3.32}$$

$$u = (\frac{M_i}{M_m}\frac{eE}{M_{im}N\sigma_0})^{\frac{1}{2}} \; for \; large \; E. \tag{3.33}$$

$$M_{im} = \frac{M_iM_m}{(M_i + M_m)} \; the \; reduced \; mass. \tag{3.34}$$

We see that for small E the drift velocity still goes as $u \propto E/p$ but for large E, $u \propto (E/P)^{1/2}$ Hence we have $u_{ion} \ll u_e$ and $u_{ion} < v_e(at \; equilibrium)$

3.3.5 Mobility

The mobility is related to drift velocity(u) as

$$u = \mu E \tag{3.35}$$

for weak fields μ is independent of E, as $u \propto E/P$, which implies that if P is a constant, then μ is a constant . But for large fields the mobility is dependent on electric field. The mobility is related to the diffusion coefficient for the Einstein relation

$$\frac{D}{\mu} = \frac{kT}{e} \tag{3.36}$$

As compared to the corresponding thermal velocities the drift velocity is slow. Typically $\mu \approx 10^{-4} m^2/Vs$

3.3.6 Modifying charge inside the gas: Recombination and Attachment

- The recombination collision rate R($m^{-3}s^{-1}$) and the recombination coefficient $\alpha(m^3 s^{-1})$ are defined such as

$$R = -\frac{dn^+}{dt} = -\frac{dn^-}{dt} = \alpha n^+ n^- \tag{3.37}$$

  with n^+ and n^- being the volume charge densities.The recombination can be Columnar recombination, where the ions and electrons from the same track recombine, thus independent of the irradiation rate, or, volume recombination, where the ions and electrons from different tracks can recombine, thus dependent on the irradiation rate.

- The attachment corresponds to the process where the electron created in the ionization process can be fixed by a neutral atom to form a negative ion. This is strongly dependent on the type of gas used, thus it is prominent process in the gas mixtures containing electronegative gasses.

The collisions that the electrons and ions undergo inside the the gas can lead to recombination (neutralization of the ion) and to attachment (the electron being captured by a neutral molecule), but another possibility is that of a charge transfer where an ion can transfer its

charge to a neutral molecule or atom. Ion-electrons pairs will generally recombine, emitting a photon in process,

$$X^+ + e^- \longrightarrow X + h\nu \tag{3.38}$$

This is different for some molecular ions, where a similar recombination reaction occurs

$$X^- + Y^- \longrightarrow XY + h\nu \tag{3.39}$$

The rate of recombination depends on the concentration of +ve and -ve ions

$$dn = bn^- n^+ dt \tag{3.40}$$

where b depends on the type of the gas used and is a constant, n^- and n^+ are the respective concentrations of -ve and +ve ions. For $n^- = n^+ = n$ integrating equation (3.40) yields

$$n = \frac{n_0}{1 + bn_0 t} \tag{3.41}$$

with n_0 is the initial concentration at $t = 0$
The *attachment* of free electrons by the electronegative atoms forms negative ions,

$$e^- + X \longrightarrow X^- + h\nu \tag{3.42}$$

The energy released in this process is called *electron affinity* as the electronegative atoms become more stable after the capture of an electron. So, the presence of an electronegative gas $(like\ O_2, H_2O, CO_2, CCl_4, SF_6)$ inside the detector severely affects the detector efficiency by capturing the electrons.

3.3.7 Avalanche Multiplication

Due the electric field present in the gas detector the electrons can accelerate and can gain sufficient energy such that they can cause ionize gas atoms or molecules. This process creates secondary, tertiary and many subsequent ionization, forming an avalanche. Due to the fact that electrons have greater mobility, the avalanche has a shape of a liquid drop (Fig. 3.4) with the electrons grouped near the head and the slower ions back at the tail.

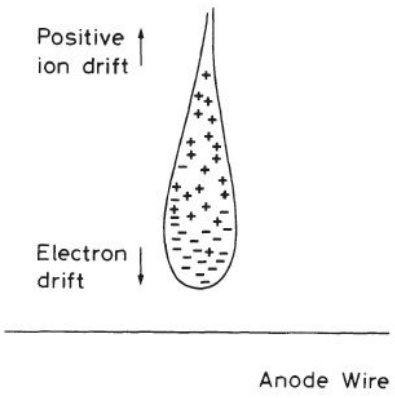

Figure 3.4: Drop Shaped Avalanche

If we consider λ to be the mean free path of the electron for later ionization events, then the probability of an ionization per path length is given by $\alpha = 1/\lambda$, where α is the *first Townsend coefficient*. We have

$$dn = n\alpha dx \tag{3.43}$$

On inegration for a path of length x equation (3.43) yields,

$$n = n_0 exp(\alpha x) \tag{3.44}$$

Then the multiplication factor (M) is

$$M = \frac{n}{n_0} = exp(\alpha x) \tag{3.45}$$

For nonuniform field configurations α is also a function of x the

$$M = exp\Big[\int_{r_1}^{r_2} \alpha(x)dx\Big] \tag{3.46}$$

This exponential can grow without limit but typically the physical limit on multiplication factor or the so called *gas gain* is about $M < 10^8$ or $\alpha x < 20$, this limit is known as *Raether limit*.

3.4 Field Intensity in a detector

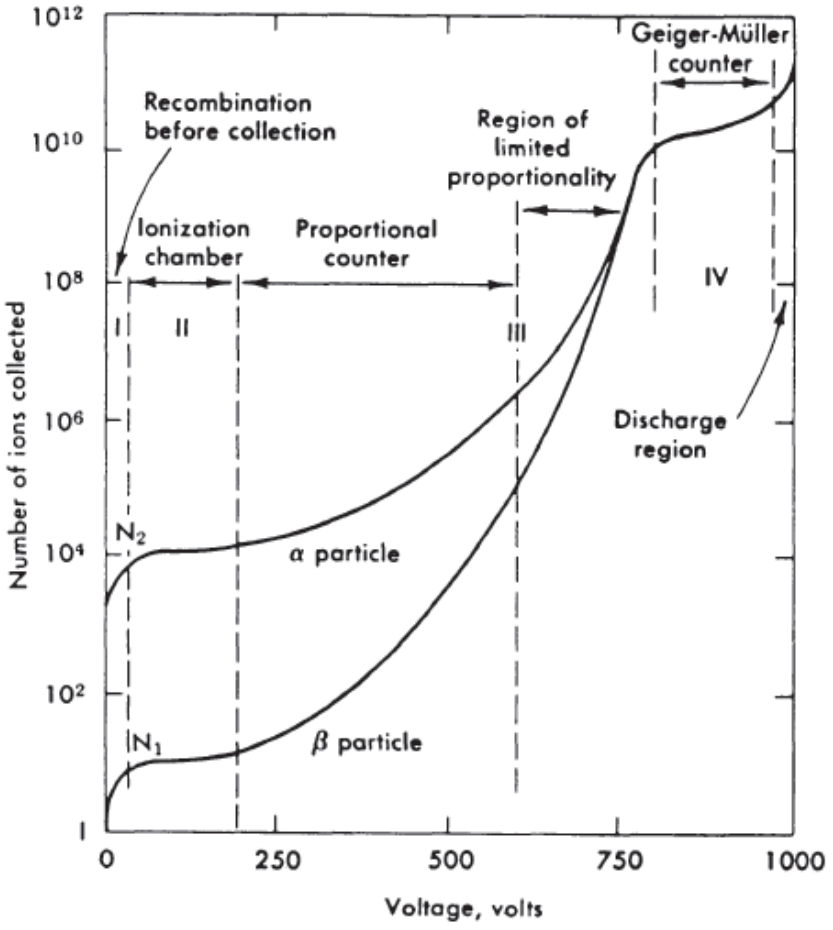

Figure 3.5: Count Rate vs Applied Voltage [Leo87]

One can see dependence on the electric field intensity by plotting number of ions collected versus the voltage applied across the electrodes. As the voltage increases the number of ions collected by the detector increases but at varying rates for different regions of the applied voltage. The detectors operated at different regions specify their specific operation for a given experimental requirement.

The different regions are (Fig. 3.5):

1. Region I

   The zero voltage point corresponds to the point where no charge is collected. The recombination dominates, hence this region is not useful for practical applications as all the electron-ion pairs produced, recombine.

2. Region II

   All the created charges are collected at some voltage and any further increase in the applied voltage has no effect. The detector operated in this region is the ionization chamber which directly collects the ions produced by the passing radiation. As the signal current is very low for the detectors operating in this region, they are usually used in current mode and are only used in large fluxes of γ irradiation.

3. Region III

   There is strong enough electric field to accelerate the freed electrons to such an energy at which they can ionize surrounding gas molecules. This creates a avalanche with subsequent ionization of gas molecules with the electrons produced in the previous ionization events. This is the amplification of the current, where the number of pairs produced in the avalanche is directly proportional to the number of primary electrons produced in the initial ionization events. So, the region is called as the proportional region and the detectors operating in this region are called the proportional counters.

4. Region IV

   As the voltage is further increased the avalanche are so large that the space charge so produced distorts the electric field at the anode, thus the proportionality is lost. This region is called as the region of limited proportionality where no detectors are operated. This region is characterized by a plateau over which there is little variation in the count rate.

5. Region V

   If the voltage is further increased, the energy that the electrons gain while accelerating becomes so large that discharge occurs in the gas. The UV radiation from the de-exciting molecules maintains the discharge by creating further ionization. Thus the output current saturates and its amplitude remains constant regardless of the energy of the initial event. The detectors which operate in this region are called the Geiger-Muller counters or Geiger counters.

6. Beyond Region V

   On further increase in the voltage there is a point where breakdown occurs with or without the presence of external radiation. As the detector can be damaged in this region, so, this region is avoided.

In general there is no single detector that can work in all the voltage regions, each type has its own geometry, gas type and other characteristics.

3.5 Types of gaseous ionization detectors

All the types of Gaseous Ionization detectors have the same basic design with two electrodes separated by a gaseous medium. The method used to measure the number of electron-ion pairs makes up for the difference. Factors like the strength of the electric field, the type of gas used to fill the detector makes the detector respond in different ways to the incoming radiation. The three types are essentially the same device working under different parameters and exploiting different phenomenon.

3.5.1 Ionization Chambers

These operate on a low electric field strength, such that there is no multiplication, the electrons and ions produced in the ionization process are drifted towards the respective electrodes under the influence of the electric field. As they are operated in the "ion chamber region", the current is unaffected by the voltage applied.
The measured current is of the order of $10^{-1}A$ without any precautions. These detectors are perfectly adapted as monitor for high rate X-ray and γ-ray detection.The efficiency can reach upto 100% in case of α and β particle detection. So, these detectors have a uniform response to radiation like the γ-radiation and have a high rate capability without getting the gas degraded. But, they give a low signal output and also are affected by ambient conditions.The ionization chambers are made in different geometric configurations like parallel electrodes, cylindrical coaxial electrodes or spherical concentric electrodes.

3.5.2 Proportional Counters

They have a slightly higher operating voltage than the Ionization chambers. Each initial ionization event produces a single avalanche, which at the last produces a current pulse which is proportional to the energy deposited so, it is called a "gas proportional detector"(GPD) in the proportional counting region.

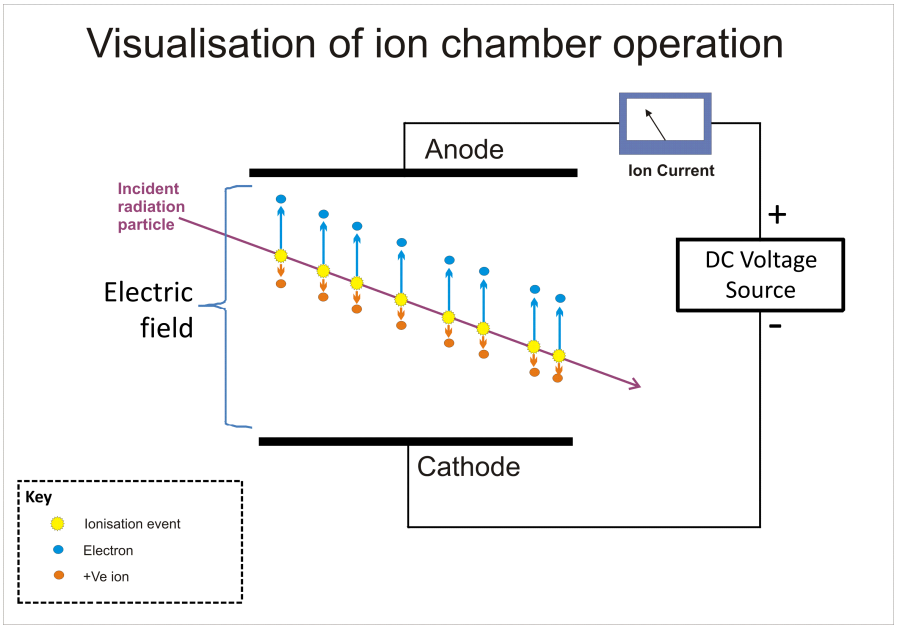

Figure 3.6: Ion chamber operation [goo]

Using these detectors we can distinguish between α and β particles as the detector provides stereographic information. The anode wires used in these detectors are delicate and lose efficiency due to deposition, which is highly probable if oxygen is present in the gas medium.

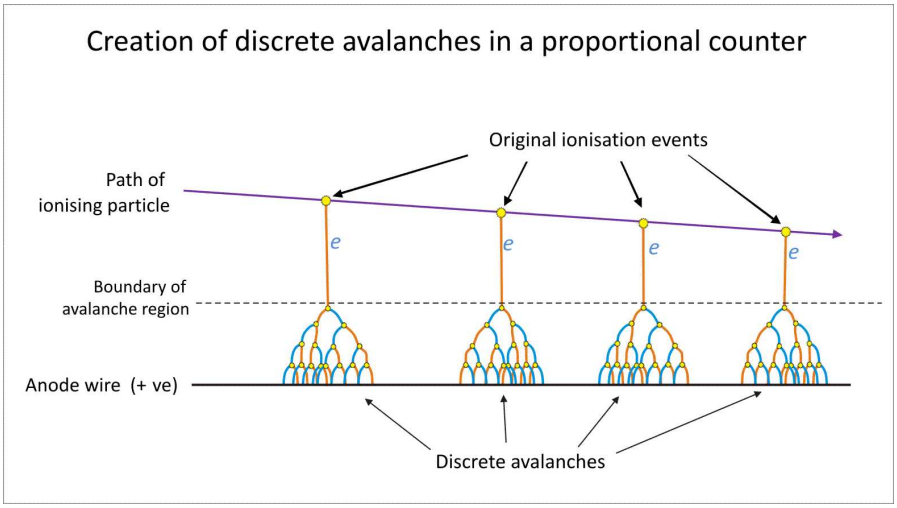

Figure 3.7: The proportional counter [goo]

3.5.3 Geiger-Muller tubes

These are the basic building blocks of Geiger counters. These are operated on even higher voltage, tuned in a way for specific needs of the experiment. There is a production of multiple avalanches along the anode wire and the region they are operated in is the ”Geiger region”.

They are cheap and good for hand held radiation detectors and also produce large signal output, reducing the need of sophisticated amplification electronics. But, these suffer from larger dead times with a faster gas degradation and do not provide any stereo-graphic information.

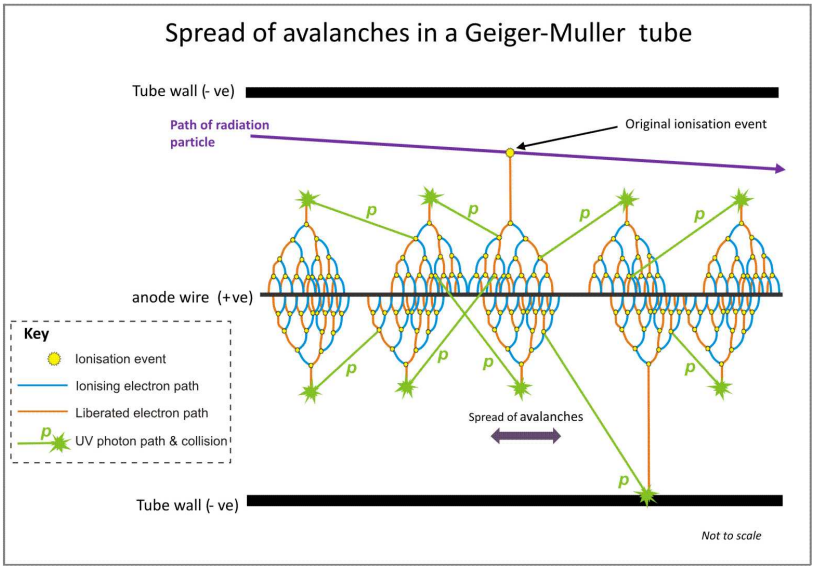

Figure 3.8: Spread of avalanches in G-M tube [goo]

3.6 The Proportional Counter

The simple proportional counters are used in the detection of low energy X-rays with energy of the order of few keV and low energy electrons from sources that can be mixed with the chamber gas. By filling the chamber with a gas of high neutron capture cross section, as in BF_3 or ^3He , then the proportional counter can be used for thermal and epithermal neutron detection. The chamber is generally filled slightly above the atmospheric pressure (to avoid atmospheric contamination), but to increase the density and thus the efficiency, higher pressures may be used.

The basic feature of a proportional counter is the proportional multiplication. The geometry of the detector is also important as it affects the field configuration inside the detector and thus affecting the gas gain and the avalanche formation. For example, for a cylindrical geometry the electric field has $1/r$ dependence and thus the field is maximum near the central wire. The higher field near the wire leads to a avalanche multiplication to occur and signal is generated. The electrons in the avalanche are collected very quickly ($\tilde{1}$ ns) while the slower ions drift towards the cathode. The ions signal is obtained only through the electrodes.

3.6.1 Shockley–Ramo Theorem

The theorem is useful to calculate the induced electric current instantaneously on a electrode due to a charge moving in the vicinity of the electrode. The instantaneous change of the electrostatic flux of the flux lines ending on the electrode produces the induced current [Sra].

This states that for an instantaneous current i induced on a electrode, the induced current value depends on the motion of charge as

$$i \; = \; E_v q v \tag{3.47}$$

where, q is the moving charge

v is the velocity of the charge at that instant

E_v is the electric field component in the direction of the movement of the charge at the instantaneous position of the charge. This has to follow some conditions (Fig. 3.9 shows a solid state detector volume, the moving charge changes the capacitance, hence the electric field inside the detector, which gives rise to an induced current):

1. the charge removed
2. unit potential applied on the electrode
3. all other conductors are grounded

3.6.2 Pulse formation and Shape of the pulse

The induced charge due to the drift of electrons and ions rather than, the charge itself is responsible for the pulse signal on the electrodes of the ionization chambers. We can

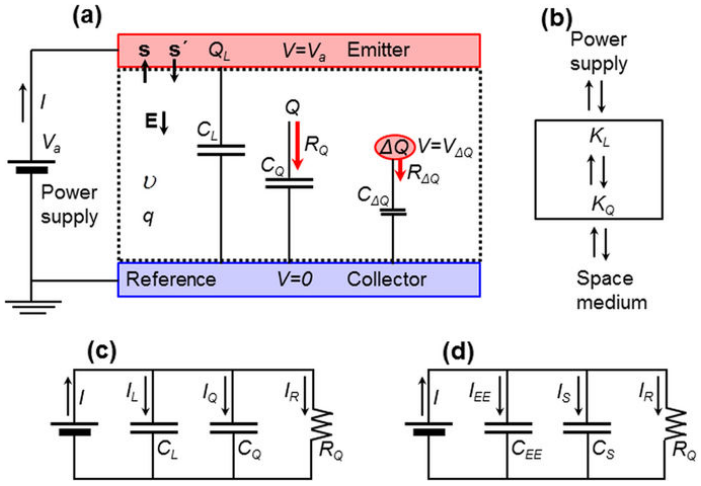

Figure 3.9: The interpretation of detector volume as capacitance (Shockley-Ramo Theorem) [goo]

simply see this in a cylindrical geometry. The electric field and potential for a cylindrical proportional counter is

$$E(r) = \frac{CV_0}{2\pi\epsilon}\frac{1}{r} \tag{3.48}$$

$$\phi(r) = -\frac{CV_0}{2\pi\epsilon}\ln\left(\frac{r}{a}\right) \tag{3.49}$$

where r is the radial distance from the central wire, V_0 is the applied potential,ϵ is the dielectric constant of the gas used, a is the radius of the wire. The capacitance per unit length of this configuration is given by

$$C = \frac{2\pi\epsilon}{ln(b/a)} \tag{3.50}$$

where b is the radius of the cylindrical chamber. Now if a charge q is located at a distance r from the central wire, the corresponding potential energy is

$$W = q\phi(r) \tag{3.51}$$

If the charge moves a distance dr, the potential energy is changed as

$$dW = q\frac{d\phi(r)}{dr}dr \tag{3.52}$$

But for a cylindrical capacitor of length l the energy contained in the electric field is

$$W = \frac{1}{2}lCV_0^2 \tag{3.53}$$

As the movement of the charges inside the chamber is relatively fast, the system can be considered closed. Then,

$$dW \;=\; lCV_0 dV \;=\; q\frac{d\phi(r)}{dr}dr \tag{3.54}$$

This results in a induced voltage across the electrodes due to the movement of charges

$$dV \;=\; \frac{q}{lCV_0}\frac{d\phi(r)}{dr}dr \tag{3.55}$$

This result is generally valid and can be used for any configuration. From equation (3.55) we can calculate the total voltage induced. Let us say that the ionization event took place and the multiplication takes place at a distance $r^{'}$ from the anode. Then the total induced voltage is

$$V^{-} \;=\; \frac{-q}{lCV_0}\int_{a+r'}^{a}\frac{d\phi}{dr}dr = \; -\frac{q}{2\pi\epsilon l}ln\big(\frac{a+r^{'}}{a}\big) \tag{3.56}$$

for positive ions,

$$V^{+} \;=\; \frac{q}{lCV_0}\int_{a+r'}^{a}\frac{d\phi}{dr}dr = \; -\frac{q}{2\pi\epsilon l}ln\big(\frac{b}{a+r^{'}}\big) \tag{3.57}$$

The total contribution to the induced voltage is $V = V^{-} + V^{+}$ and the ratio of their contribution is

$$\frac{V^{-}}{V^{+}} \;=\; \frac{ln\frac{a+r^{'}}{a}}{ln\frac{b}{a+r'}} \tag{3.58}$$

The multiplication region is limited to a distance of few wire radii, thus the contribution of electrons to the induced voltage is small compared to the positive ions [Leo87]. The induced signal is entirely due to the motion of the positive charges ans thus the motion of the electrons can be ignored(only in the case where all the electrons are created near the anode).The time development of the pulse is given as

$$V(t) \;=\; \int_{r(0)}^{r(t)}\frac{dV}{dr}dr \;=\; -\frac{q}{2\pi\epsilon l}ln\frac{r(t)}{a} \tag{3.59}$$

where r(t) is defined as

$$\frac{dr}{dt} \;=\; \mu E(r) \;=\; \frac{\mu CV_0}{2\pi\epsilon}\frac{1}{r} \tag{3.60}$$

Integrating equation (3.60) yields

$$r(t) \;=\; \big(a^2 + \frac{\mu CV_0}{\pi\epsilon}t\big)^{\frac{1}{2}} \tag{3.61}$$

with $r(0) = a$. Using equations (3.59) and (3.61) we have

$$V(t) \;=\; -\frac{q}{4\pi\epsilon l} ln\big(1 + \frac{\mu C V_0}{\pi\epsilon a^2}\big) \;=\; -\frac{q}{4\pi\epsilon l} ln\big(1 + \frac{t}{t_0}\big) \tag{3.62}$$

taking

$$t_0 \;=\; \frac{a^2\pi\epsilon}{\mu C V_0} \tag{3.63}$$

Then the total drift time T is

$$T \;=\; \frac{t_0}{a^2}(b^2 - a^2) \tag{3.64}$$

3.6.3 Choosing the Fill Gas

Factors that govern the choice of a filling gas for a proportional counter are:-

1. Low working voltage
2. High gain
3. Good proportionality
4. High rate capacity

These conditions are addressed generally using a gas mixture rather than a pure one. For lower operating voltage noble gases are used, as they require lowest field intensity to form an avalanche. Like the cost effective and with a higher specific ionization argon is used as a filling gas. But, pure argon can only be used for gains lower than $10^3 - 10^4$ without the occurrence of continuous discharge. This is due to the fact that argon has a high excitation energy (11.6 eV), so a dexcited argon atom can release high energy photons which can further produce avalanches. This hinders the proportionality property of the proportional counter and thus the gain of the detector.

This problem is addressed by adding a poly-atomic gas, such as $CO_2, BF_3, isobutane$. The poly atomic gasses thus added are called *quenchers*. Quenchers absorb the radiated photons and dissipate the energy through dissociation or elastic collisions [Leo87]. The addition of just a small amount of quencher has a drastic effect on the detector performance, indeed gains of up to 10^6 can be obtained. For example a gas mixture known as *P10* which is a mixture of 90% of Ar and 10% of methane (CH_4).

The gain can be further improved by using a judicious amount of electronegative gas such as Freon (CF_3Br). These not only absorb the high energy photons, but also trap electrons from the cathode before they can reach the anode to cause a avalanche, this can help achieve gains of the order of 10^7.

3.7 Micro pattern gas detectors

It is a class of gaseous ionization detectors which are developed for better spatial resolution and response time as a very small interaction volume is used [BAB+06]. Widely used micro pattern detectors are-

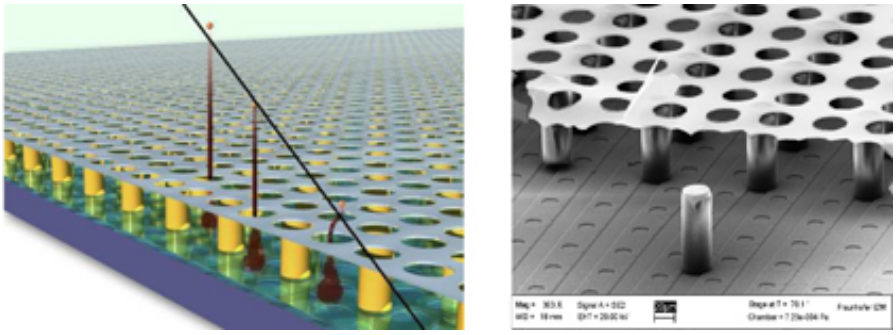

Figure 3.10: A Miro-Pattern Gas detector [goo]

3.7.1 GEM detector

A gas electron multiplier (GEM) is a type of gaseous ionization detector used in nuclear and particle physics and radiation detection[gem]. GEMs create the large electric field in small holes (Fig. 3.11) in a thin polymer sheet; the avalanche occurs inside of these holes. The resulting electrons are ejected from the sheet, and a separate system must be used to collect the electrons and guide them towards the readout. GEMs were invented in 1997 in the Gas Detector Development Group at CERN by physicist Fabio Sauli. The signal from the GEM detector is obtained from the read-out palne, which is the electron signal.

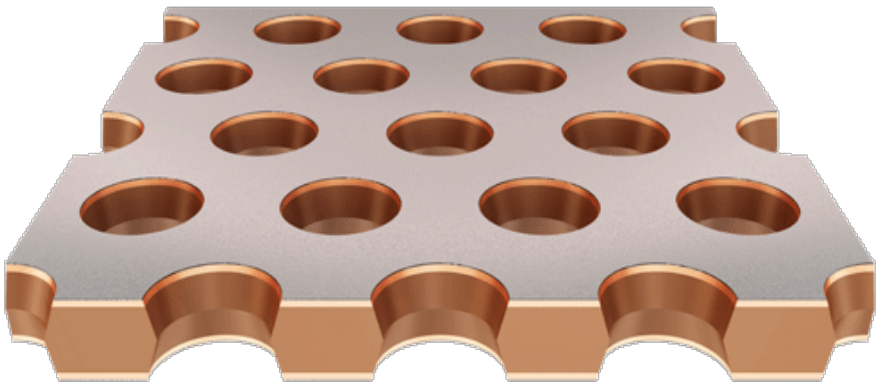

Figure 3.11: Enlarged GEM foil

3.7.2 MicroMegas detector

The “Micromegas “ (Micro-MEsh Gaseous Structure) (Fig. 3.12) detector is a gaseous ionization particle detector coming from the development of wire chamber[mic]. Invented in 1992 by Georges Charpak and Ioannis Giomataris, these are mainly used in experimental physics, in particular in particle physics, nuclear physics and astrophysics for the detection of ionizing particles. The Micromegas are light detectors in order to minimize the perturbation on the impinging particle. From their small amplification gap, they have fast signals in the order of 100 nanoseconds. They are precise detectors with a spatial resolution below one hundred micrometers. Nowadays, the use of the Micromegas technology is growing over the different fields of experimental physics. The signal from a micromegas detector can be obtained from the micromesh, the ion-signal and from the read-out plane, the electron signal.

3.7.3 Some features that make micro-pattern detector an ample choice for X-ray detection [BBB$^+$03, BBB$^+$06, BBC$^+$13, BM10]:

1. Can work over a wider temperature range.
2. Minimum perturbation on the impinging particles.
3. High spatial resolutions (typically $\sim 50\ mm$).
4. Very fast read out (in 100 ns)

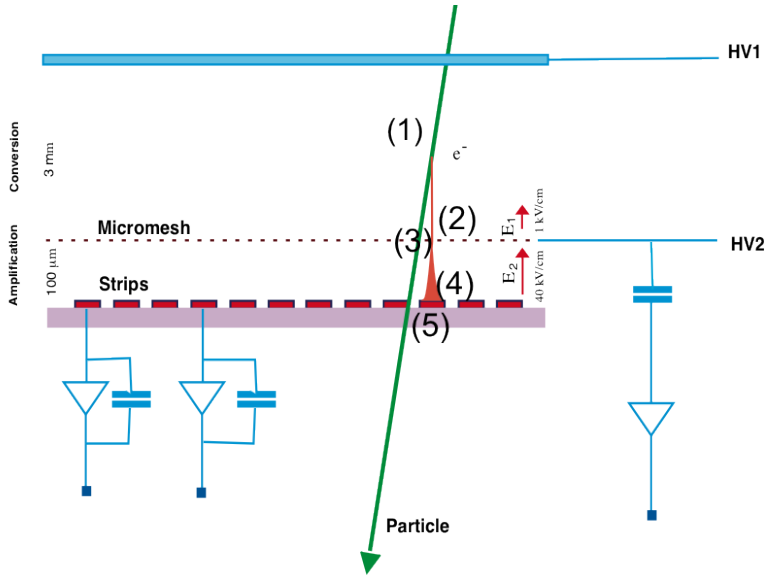

Figure 3.12: Micromegas Detector [goo]

5. High Rate capability few MHz/mm^2.

6. Can be optimized to cover wide X-Ray band (100eV to 100keV and more)

7. Can do Polarization study effectively with 2-D readouts.

These features make them a good detector for the use in X-ray astronomy. In the next chapter simulation tools and strategies have been discussed, so as to test the idea in-silico. In the next chapter discusses the tools for the detector simulation. [Literature studied from [DTF03],[Kno89],[STY10]]

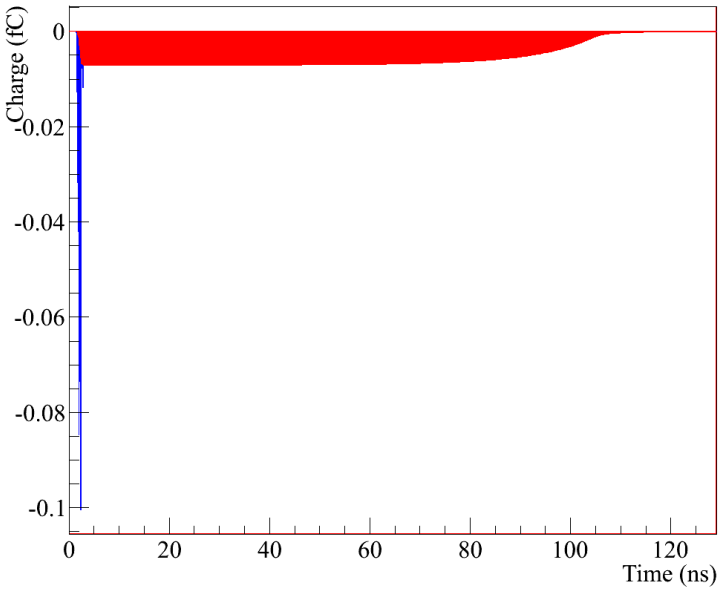

Figure 3.13: Signal from a micro-megas detector, blue color : electron signal, red color : ion-signal [goo]

Chapter 4

Simulation tools and strategies

4.1 Introduction

The computer simulations are able to reproduce behavior and properties of a system based on some mathematical models and formulation. For doing a simulation the first question to ask is what the system is and what the user seeks from the simulation results. Preparing a prototype and testing it is a tedious task which not only involves use of a lot of resources but can be wasteful if the desired results are not obtained. Simulations help to make this process less time and resource consuming. They help us to check the working of the system by working on a virtual model. This helps to encounter problems that can arise in a real prototype and to solve them a priori. Here in this work we want to simulate a Micromegas detector and see if it can be used for X-ray imaging of celestial objects. For the purpose of simulating a Micromegas detector we need to address following:

1. Define the detector geometry and simulate the geometry
2. Define the applied voltage on different components of the detector
3. Define the Gas mixture inside the detector and check various gas properties for the gas
4. Check the electric field inside the the detector volume
5. Check the drift properties for the gas medium
6. Pass a radiation particle through the detector

7. See the response of the detector for the passage of the particle
8. Collect the signal from the detector
9. See if the signal is meeting the theoretical expectations
10. Characterize and optimize the detector operation by tweaking the detector geometry, components and the gas mixture for the specific use.

4.2 Simulation tools

To address the issues listed in section (4.1) regarding the simulation of Gaseous Ionization detectors (in general), using the following tools

4.2.1 Garfield

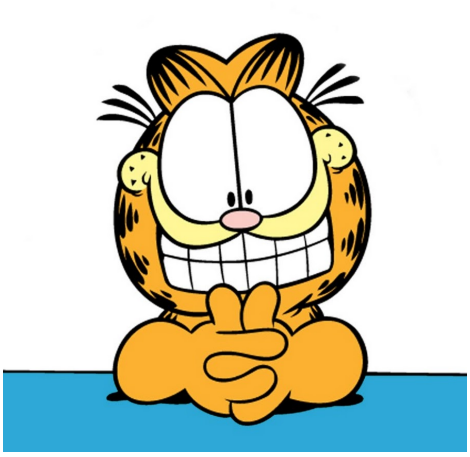

Figure 4.1: Garfield the cat [goo]

Garfield is a computer program developed by Rob Veenhof at CERN for the purpose of simulating 2D and 3D drift chambers and gaseous ionization detectors [Vee]. The program can calculate the following:

1. field maps, contour plots and 3-dimensional impressions;
2. the wire sag that results from electrostatic and gravitational forces;
3. optimum potential settings to achieve various conditions;

4. plots of electron and ion drift lines;

5. x(t)-relations, drift time tables and arrival time distributions;

6. signals induced by charged particles traversing a chamber, taking both electron pulse and ion tail into account.

Garfield can simulate gaseous ionization detectors by integrating programs discussed below in sections (4.2.2, 4.2.4, 4.2.3).

4.2.2 neBEM

neBEM computes the electric field and potential in nearly arbitrary 3D geometries taking into account the presence of conductors and dielectric media. This program takes the cell or geometry definition from the Garfield and returns the corresponding electric field and potential configuration that can be used in the initialization of the chamber. It also takes into account the potentials at which the different chamber components are kept.[SM]

4.2.3 Magboltz

Magboltz solves the Boltzmann transport equations for electrons in gas mixtures under the influence of electric and magnetic fields. This helps to simulate the transport properties of the gas used in the detector, which helps in studying the response of the gas medium in the detector under the applied fields. Magboltz simulates the transport of the electron form the site of their creation , when the incident radiation interacts with the gas medium to the signal electrodes of the detector.[Bia]

4.2.4 Heed

Heed simulates the interaction of radiation particles with gases. Heed calculates in the energy loss of charged particles in gases, by taking δ electrons and optionally multiple scattering that the incoming radiation particle into account. The absorption of photons through photo-ionization in gaseous ionization detectors can be simulated.[Smi] The program can calculate quantities as:

1. Number of clusters per cm

2. Cluster size distribution

3. Range and straggling of delta electrons

Heed interfaced with Garfield can provide us the properties of interaction between the incoming radiation and the gas particles inside the detector, which is a essential for knowing the detector response to the radiation.

4.3 Simulation technique

We can use Garfield to simulate the Micromegas detector and to study how it responds to the X-rays from celestial sources. Following are the steps involved in that:

1. Define the cell geometry in Garfield and calculate the electric field and potential configuration using the neBEM interface

2. Define the gas medium inside the chamber and define its transport properties, which Magboltz can do.

3. Make a X-ray photon go through the detector and interact with the detector's gas medium, which is handled by the Heed interface.

4. The Garfield can then take simulate the signal acquisition from the selected electrodes.

The Garfield code structure and the simulation results are discussed in the next chapter.

Chapter 5

Simulations and Results

The simulations were carried out on Garfield.[Vee] The task was to simulate the detector as close as possible to the actual physical parameters. Following sections discuss the simulations and corresponding results.

5.1 Geometry section

The first task is to construct a geometry for the detector, including the voltages applied on different components of the detector. The simulations can be very time consuming (CPU time) so its better to work on a section of the geometry. The section has to be chosen in such a way that the dynamics for the full scale detector can be inferred from that section effectively.

The detector to be simulated was the Micromegas detector, so the section considered for the simulation was a 9-cell micromesh out of a half a million in an actual detector. Considering the uniform periodicity of the cell geometry leads to a good approximation of the actual detector physics. This even eliminates the boundary effects that can come due to the fact that the geometry considered is very small as compared to the actual detector geometry.

Micromegas can be constructed in two basic configurations depending on the elements on which the voltages are applied. This is critical to the functioning of the detector as this changes the field configuration inside the detector. For a micromegas we need a drift plane, a micromesh, readout plane and a cathode plane. The choice of application of the voltages on different parts of the detector decides the configuration of the detector.

The two configurations considered for the simulations are :-

5.1.1 First Configuration

In the first configuration is the one in which a *-ve drift voltage (DC) is applied on the drift plane* and a *+ve amplification voltage (DC) is applied on the read-out plane*. This produces a gradient inside the chamber and produces an electric field in a direction away from the read-out plane and into the drift plane. This configuration uses a +ve and -ve DC voltage application on the opposite ends of the detector hence getting a proper field configuration is a bit easier.

This configuration also has a problem that if the +ve amplification voltage (DC) is applied directly on the read-out plane then the noise can be introduced in the signal due to the HV supply. This problem is addressed by using resistive strip at a +ve potential instead of a read-out plane. The signal then acquired is from the read-out strips, which are separated form the resistive strips using a thin layer of an insulating material. This configuration is better for a strip read-out geometry.

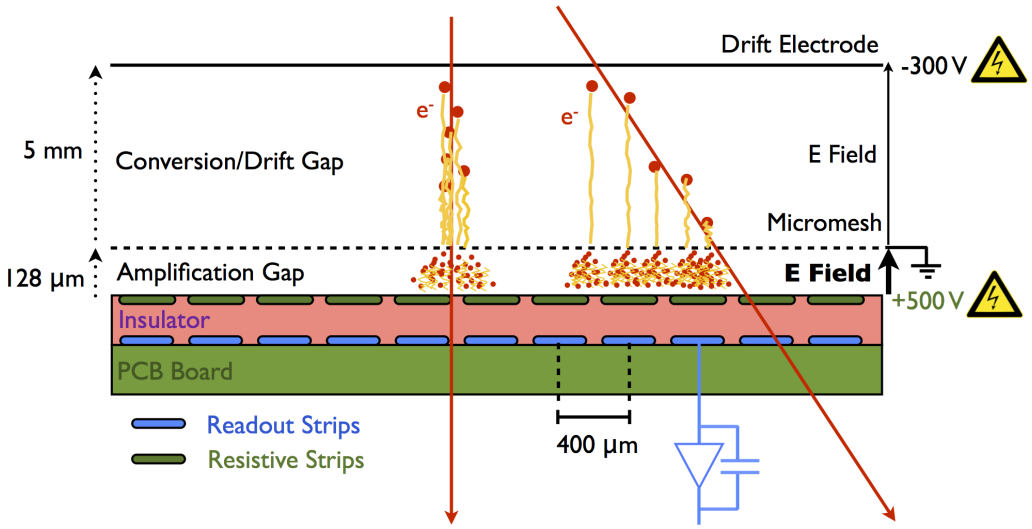

Figure 5.1: The first configuration with the amplification voltage applied on the resistive strips in the read-out plane

5.1.2 Second Configuration

In the second configuration is the one in which a *-ve drift voltage (DC) is applied on the drift plane* and and a less -ve *amplification voltage (DC) is applied on the micromesh*. This produces a gradient inside the chamber and produces an electric field in a direction away

from the read-out plane and into the drift plane.

This configuration poses a little bit of a problem as the voltage applied on the micromesh is also negative, hence requires a very good tweaking so that the electrons and the ions produced inside the detector by the ionizing radiation are drifted properly towards the readout and the drift plane respectively. This has also a advantage that the application of a high voltage is separated from the read-out leading to a lower noise even with a high noise DC voltage supply. If tweaked in properly this configuration can be used effectively. This configuration is better for the padded read-out structure as we can expose the read-outs directly to the incoming avalanche.

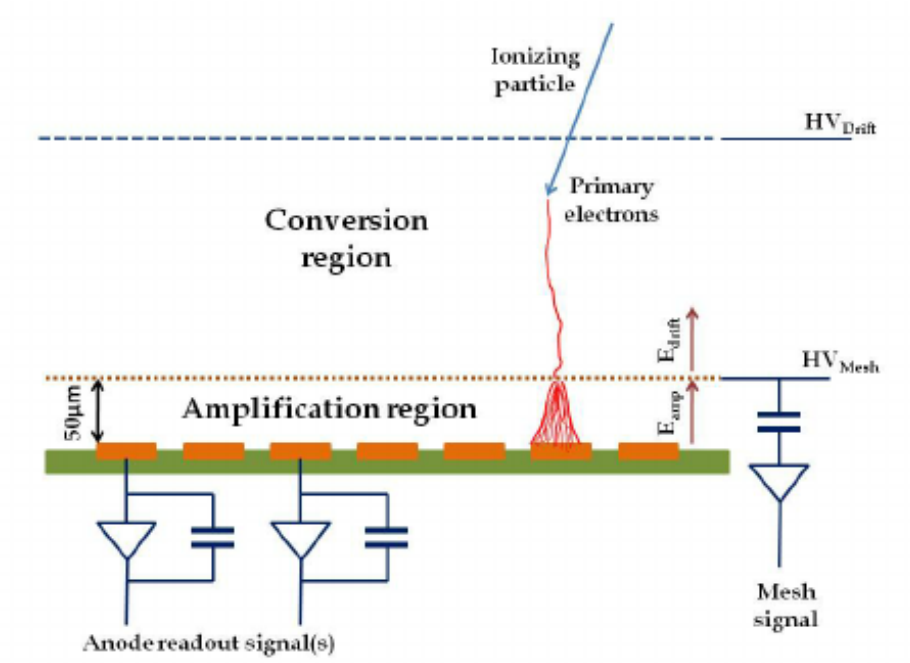

Figure 5.2: The second configuration with the amplification voltage applied on the micromesh

5.1.3 Geometry Implementation in Garfield

In Garfield simulation code the **"&CELL"** section is the part where the geometry is defined for making elements in the simulation, **"solids"** command is used, under which we can define *"boxes, wires and the material of which they are made"*. The interface of Garfield with the **"neBEM or near Boundary Element Method"** is used to calculate the charges

induced on, potential and electric field in different components of the detector, which is dicussed earlier in section (4.2.2)

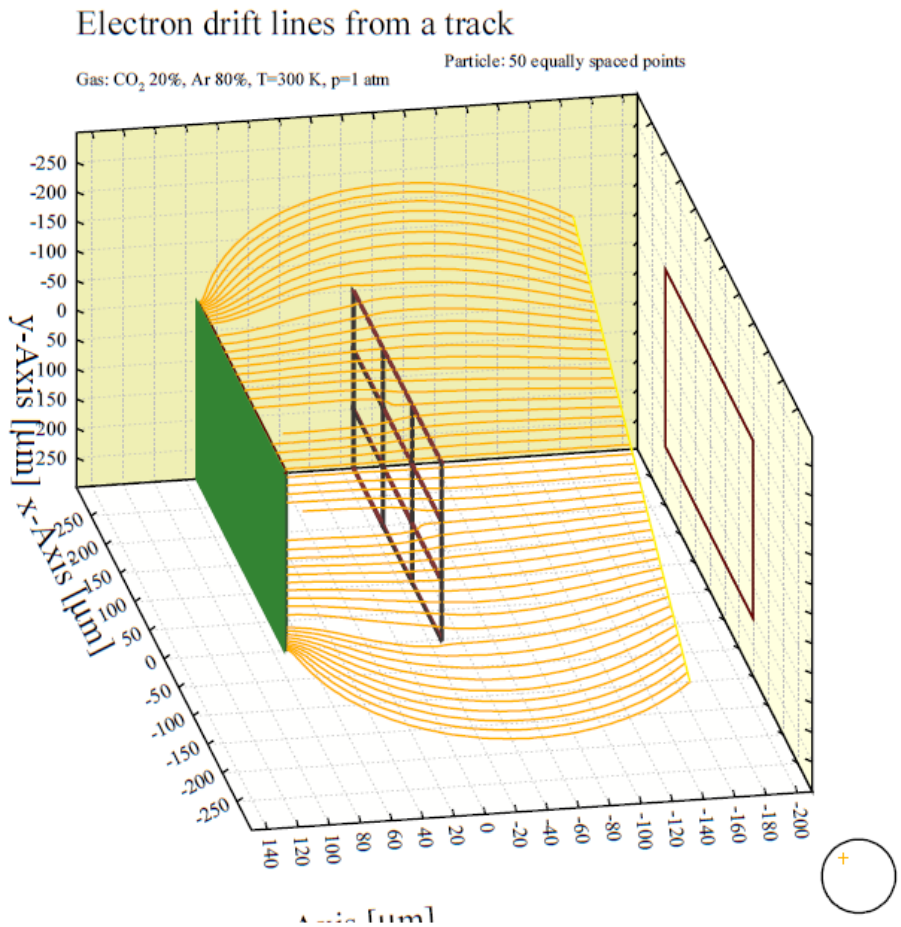

Figure 5.3: Basic geometry consisting of a micromesh, a drift plane and a read-out plane (in green), the figure also shows the drift lines (yellow lines) for 50 electrons

5.1.4 Field section

The field configuration inside the detector is very important to consider as discussed earlier in section (3.4). The field configuration can be simulated in the Garfield package under the **"&FIELD"** section, where the *Potential contours, electric filed strength along a defined axis of the detector and the vector field plot.*

This helps in optimizing the field configuration so that the desired detector operation can be simulated. Once the geometry and corresponding voltages on the detector components are defined the field configuration is fixed. So, this depends on the definition of the geometry

in the ”&CELL” section of the Garfield code. The plots for the field and potential configuration are obtained using the **”neBEM or near Boundary Element Method”** interface with the Garfield.

5.2 Gas section

The gas used inside a gaseous ionization detector is very important to consider as discussed in the section (3.6.2). The gas used decides the use of detector in the detection of different kinds of radiation. For the detection of different kinds of radiation the gas mixture has to optimized.

For the simulation of Gas medium inside the detector Garfield uses the interfaced **”Magboltz”**(section 4.2.3), which simulates and calculates the transport properties of electrons and ions in the gas medium. The **”& GAS”** section in a Garfield code is the section where the gas medium to be used in the simulation can be defined.

5.3 Drift section

The drift section or the **”&DRIFT”** section in Garfield is used to define the simulation parameters for the drift of the electrons and ions in the gas medium. This uses the gas properties computed by Magboltz in the &GAS section. Using this section we can simulate electrons drifting along the electric field lines or effectively on the drift lines. The section uses the Monte-Carlo simulation to integrate the drift lines considering the field and gas properties of the gas chamber. This helps in checking for any inconsistencies in the electric filed or the detector geometry that can interfere in the electron drift inside the detector. This helps in the optimization of the detector.

5.3.1 Signal section

The information about the incident radiation is obtained through the induced or direct signal obtained form the drift of charges inside the chamber or the hit of actual charge carriers on the detector components. The signal is obtained in form of a pulse as discussed in the section (3.6.1).

The drift of the ionizing radiation and its interaction with the gas medium is simulated using

the **"HEED"** interface with Garfield. The interface also takes into account the ionization, excitation and attachment. The signal is calculated according to the Shockley–Ramo Theorem (3.6.1) on the read-out plane or strips. The induced charge on the read-out strips or the direct charge deposition is then calculated using Monte-Carlo simulation by Garfield. The Garfield then provides the information about the pulse formation along with the actual drift timings and the number of clusters formed using the HEED interface.

5.4 The Simulations and Results

5.4.1 The geometry

Both the geometries (5.1.1 and 5.1.2) were considered in the cell geometry simulations as shown in the figures (5.4) and (5.5)

The first geometry parameters (Fig. 5.4):

1. Drift plane: 0.175mm $\times$ 0.175mm
2. Drift gap : 2.5mm
3. Amplification gap : 0.1mm
4. Drift Voltage: -300 V
5. Amplification Voltage: +500 V , applied on the read-out plane
6. Mesh size : 9 cells, 0.175mm $\times$ 0.15mm
7. Read out plane: 0.175mm $\times$ 0.175mm

The second geometry parameters(Fig. 5.5):

1. Drift plane: 0.175mm $\times$ 0.175mm
2. Drift gap : 2.5mm
3. Amplification gap : 0.1mm
4. Drift Voltage: -500 V

5. Amplification Voltage: -300 V , applied on the micromesh

6. Mesh size : 9 cells, 0.175mm $\times$ 0.15mm

7. Read out plane: 0.175mm $\times$ 0.175mm

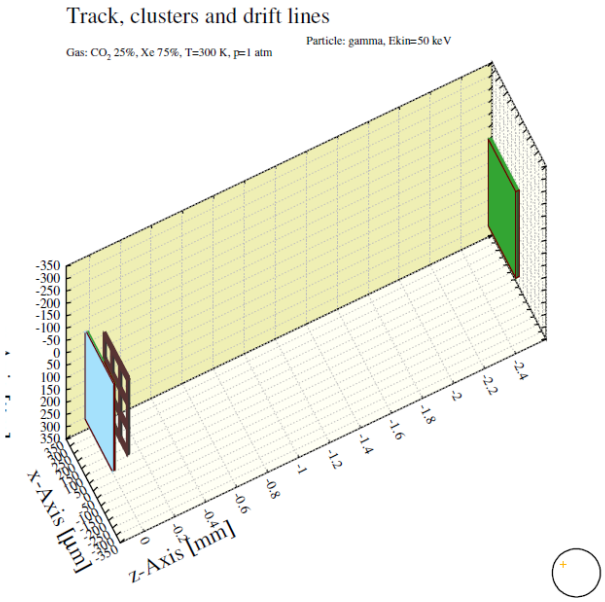

Figure 5.4: The first configuration simulation

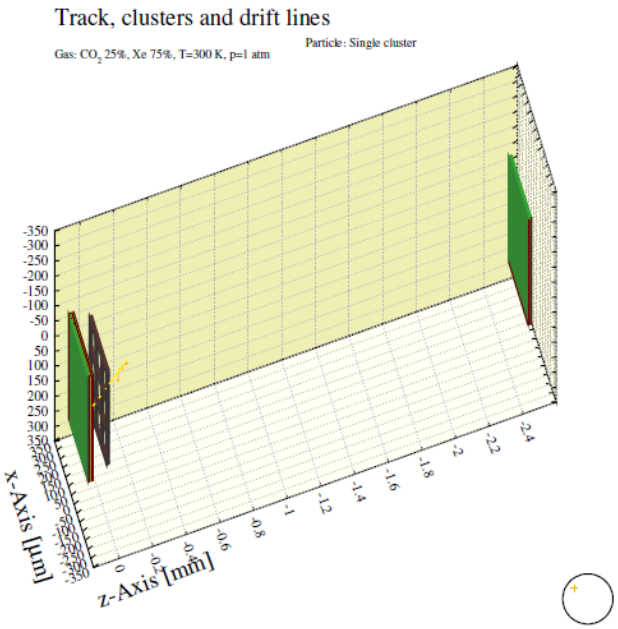

Figure 5.5: The second configuration simulation

The field configuration simulations for the chamber (A magnified view)

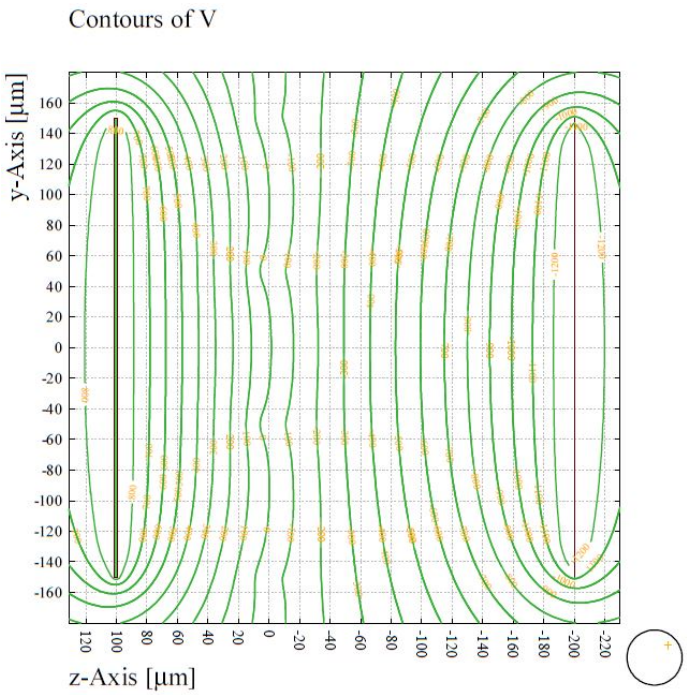

Figure 5.6: The potential contours

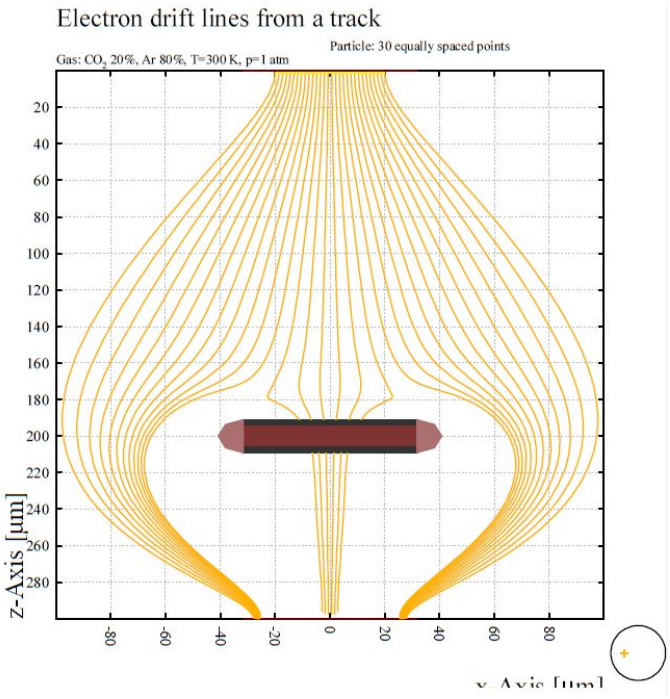

Figure 5.7: Drift of a cluster of electrons inside the chamber

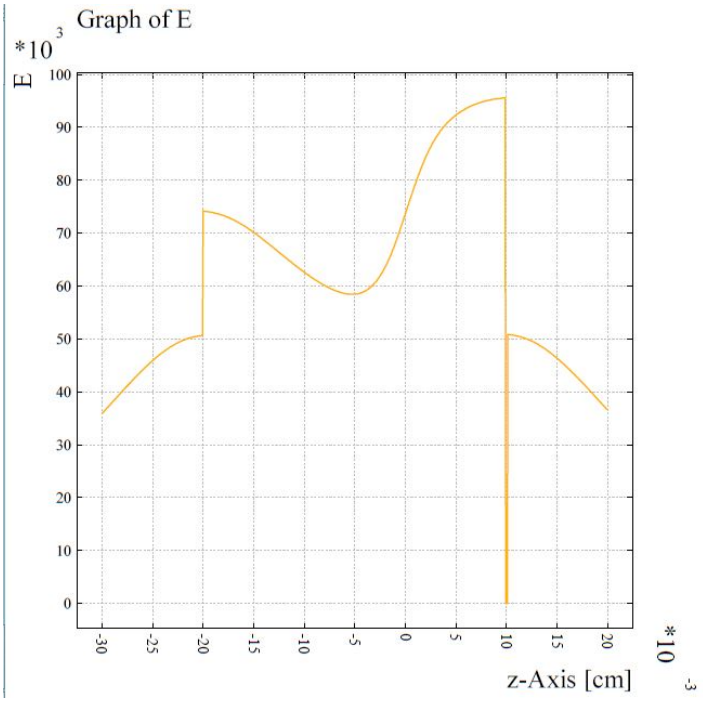

Figure 5.8: The electric field intensity along the axis of the detector

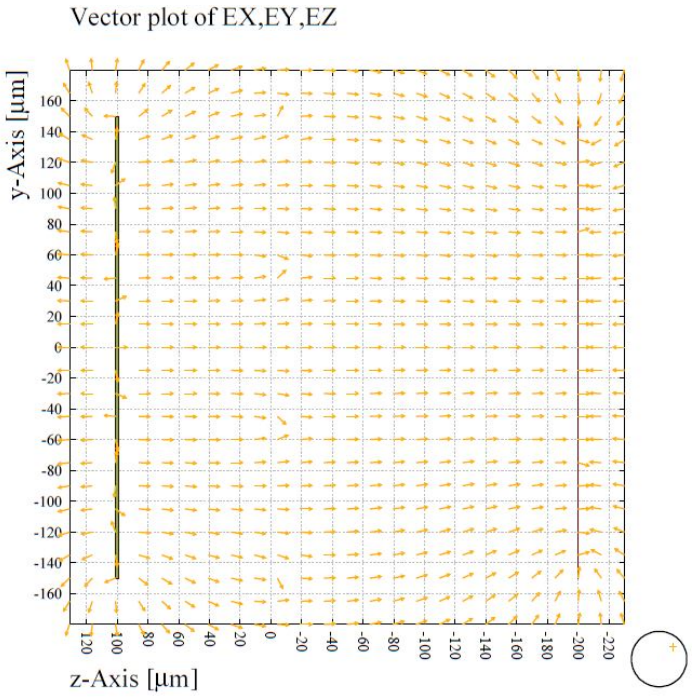

Figure 5.9: Electric field vector plot

5.4.2 The Gas

Gas mixtures that were used are as follows:

1. Pure Isobutane
2. Neon and DME in a 4:1 ratio
3. Argon and CO_2 in a 4:1 ratio
4. Xenon and CO_2 in a 3:1 ratio

The properties of the gas mixtures simulated by Magboltz are shown below

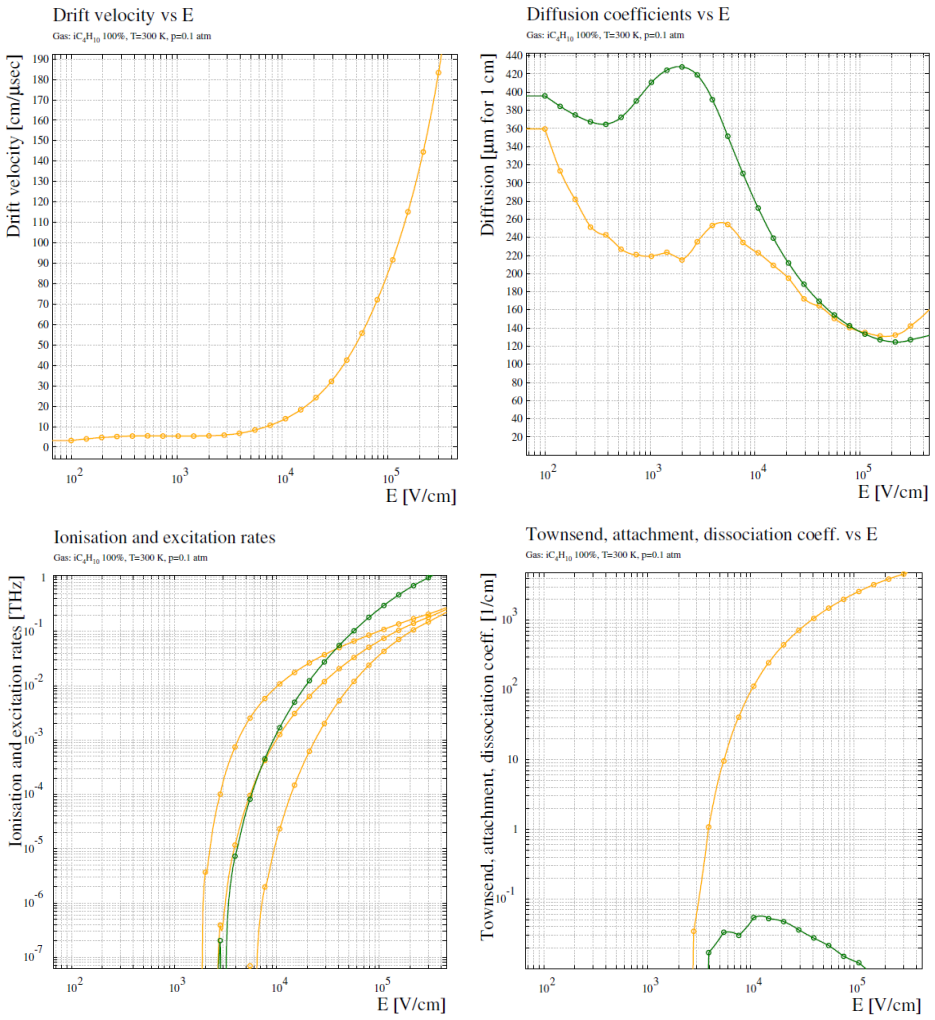

Figure 5.10: Gas properties for pure isobutane (iC_4H_10) at 0.1 atm pressure

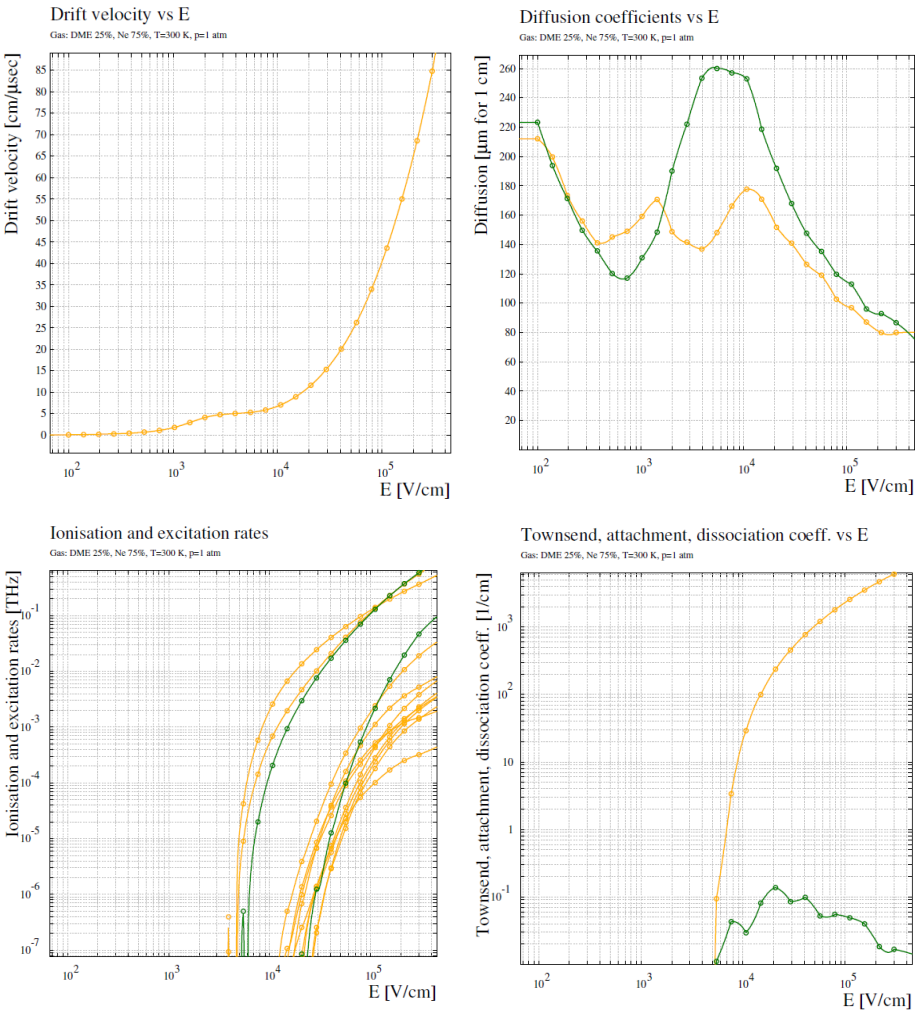

Figure 5.11: Gas properties for Ne and DME gas mixture in 4:1 ratio at 1 atm pressure

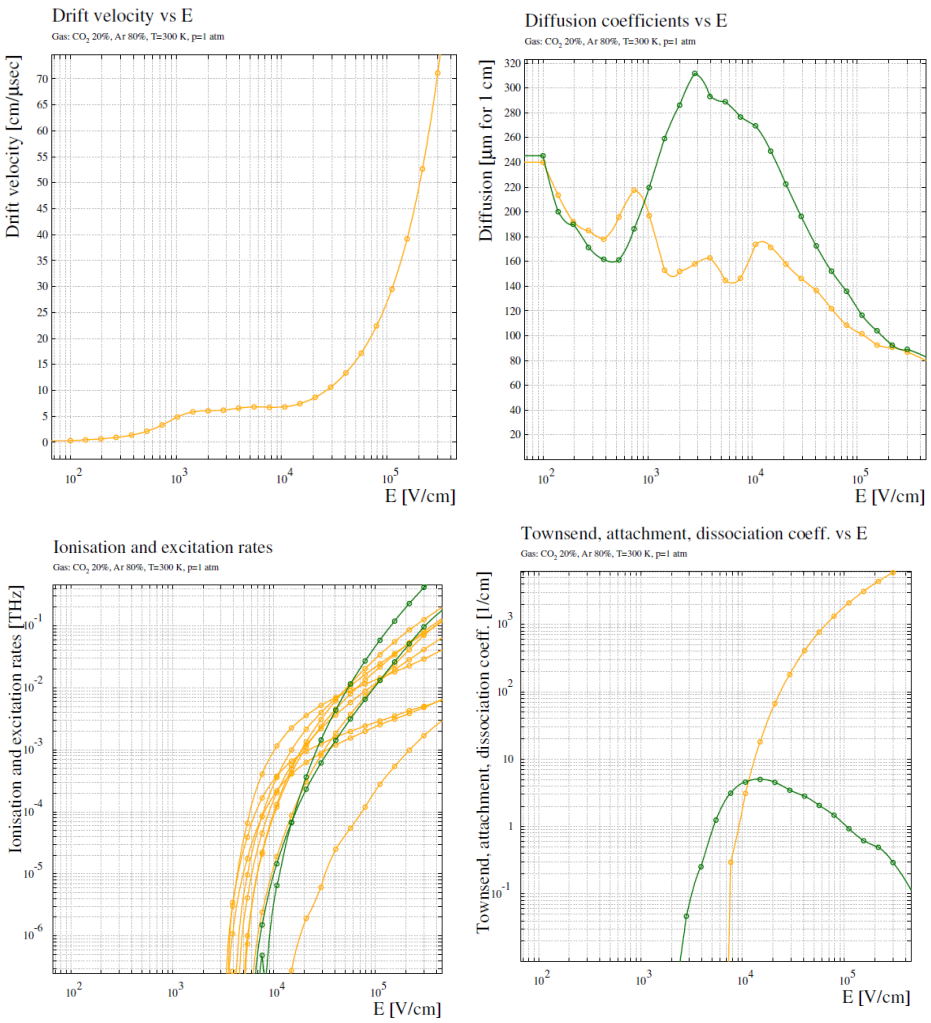

Figure 5.12: Gas properties for Ar and CO_2 gas mixture in 4:1 ratio at 1 atm pressure

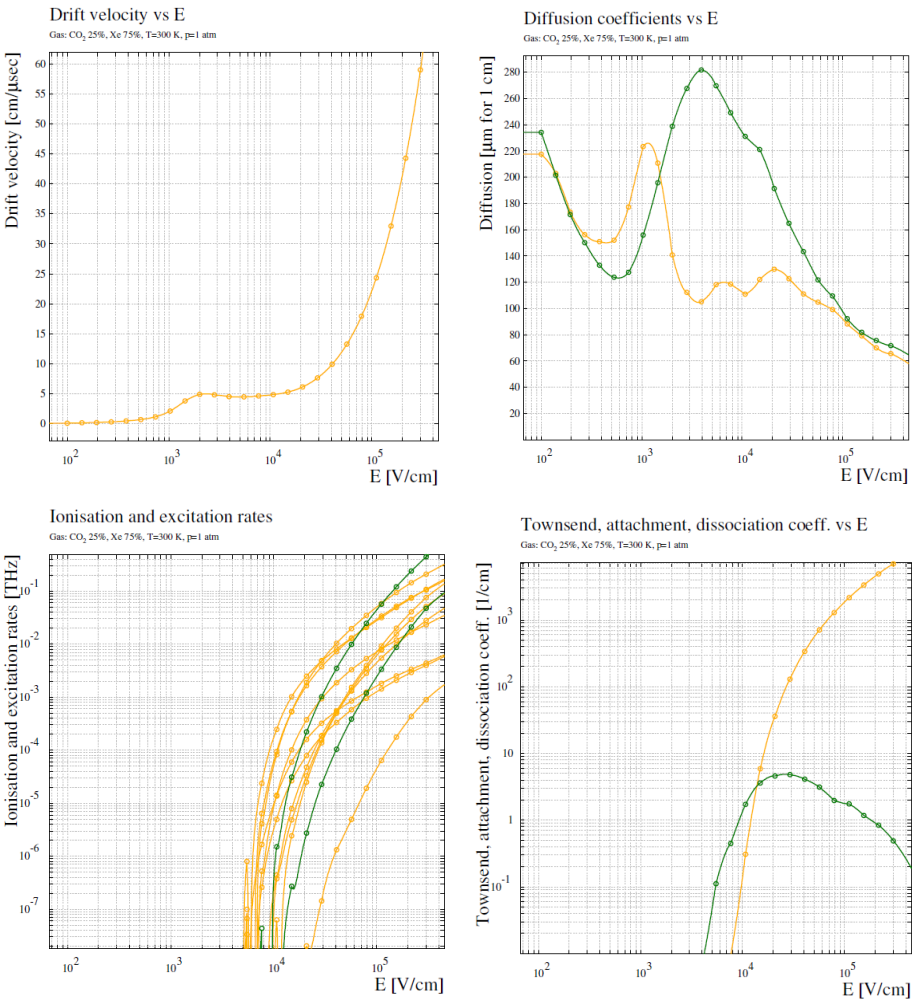

Figure 5.13: Gas properties for Xe and CO_2 gas mixture in 3:1 ratio at 1 atm pressure

The Passage of Ionizing radiation and the corresponding signal obtained:

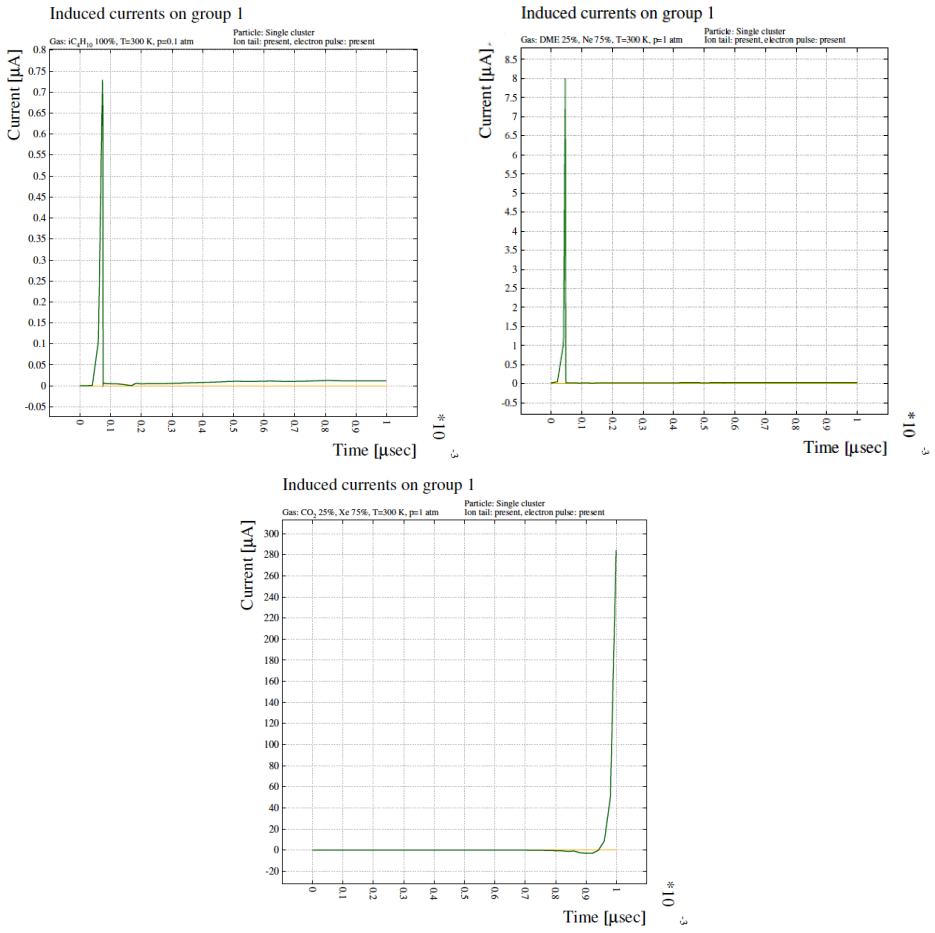

Figure 5.14: Signal obtained using geometry 1 by passing a 1KeV X-ray photon

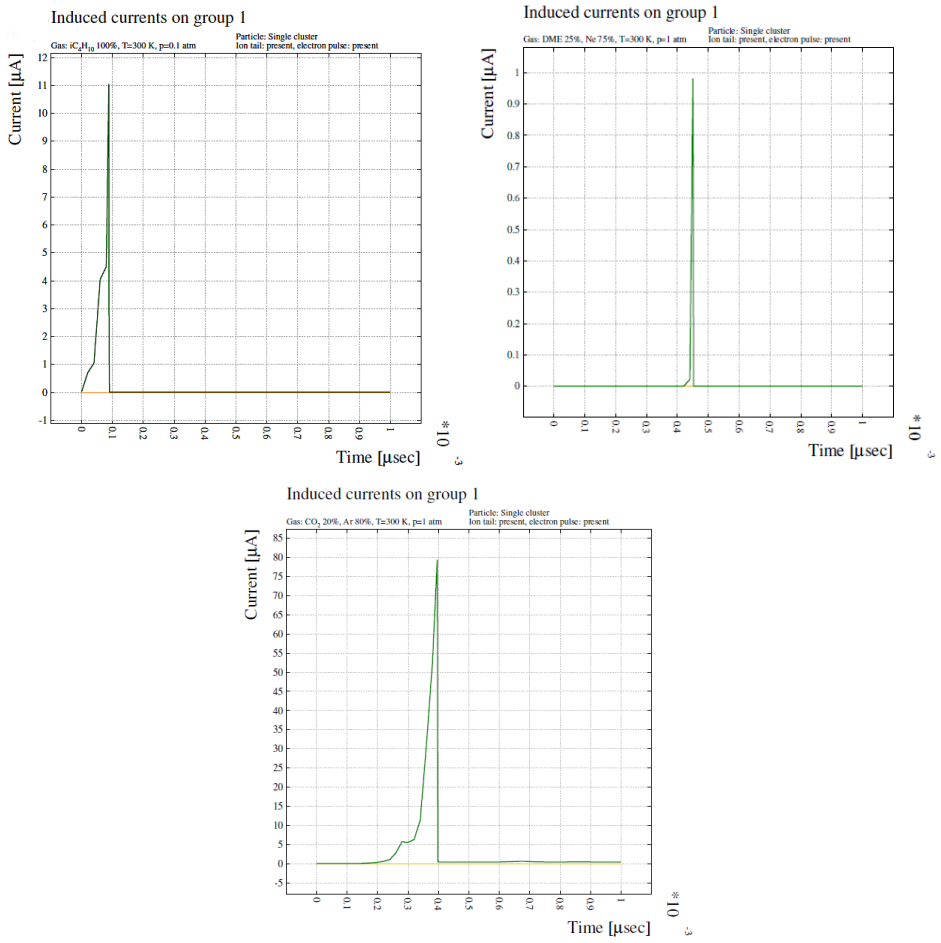

Figure 5.15: Signal obtained using geometry 1 by passing a 10KeV X-ray photon

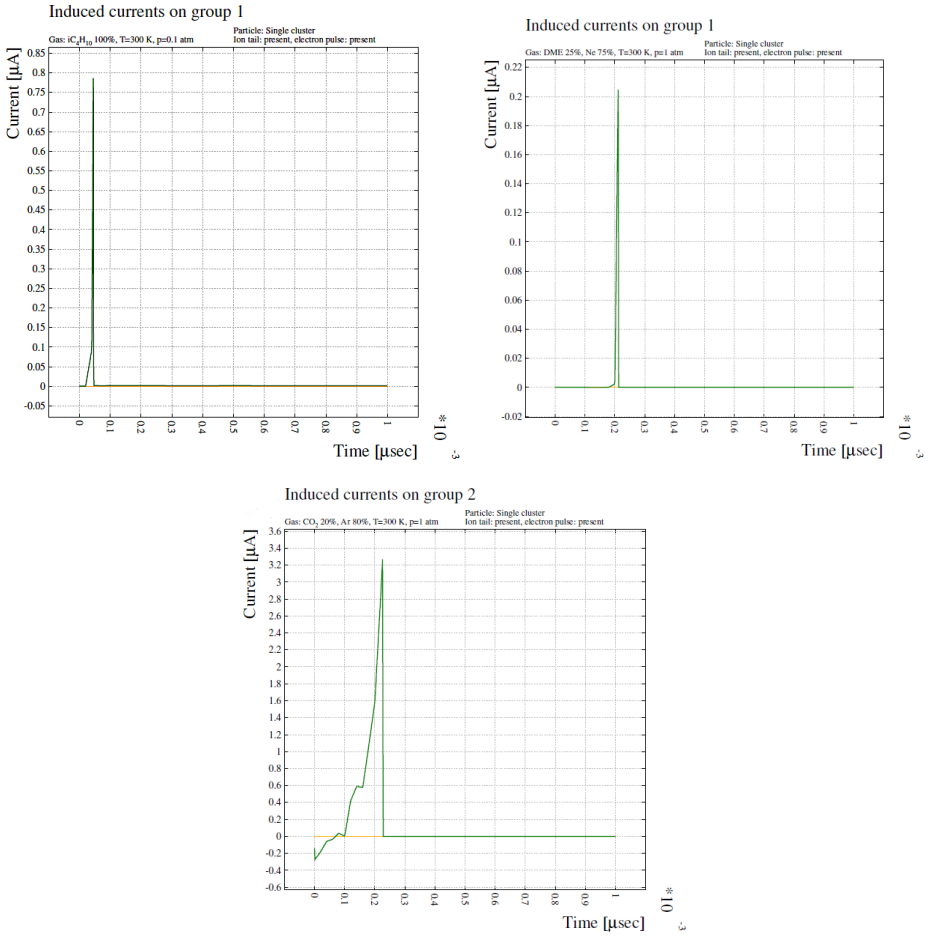

Figure 5.16: Signal obtained using geometry 1 by passing a 50KeV X-ray photon

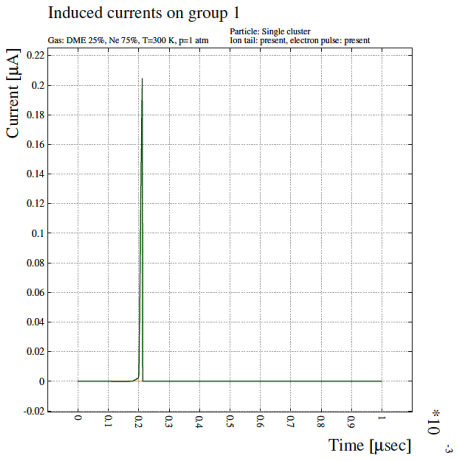

Figure 5.17: Signal obtained using geometry 1 by passing a 90KeV X-ray photon

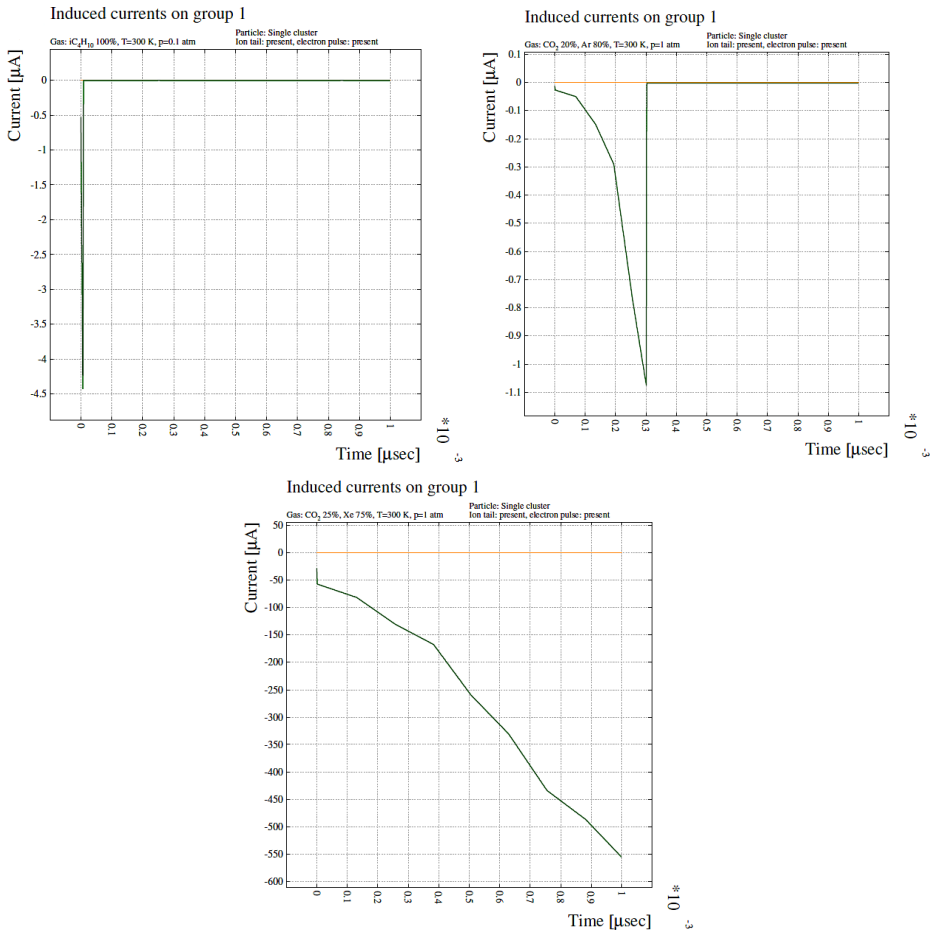

Figure 5.18: Signal obtained using geometry 2 by passing a 1KeV X-ray photon

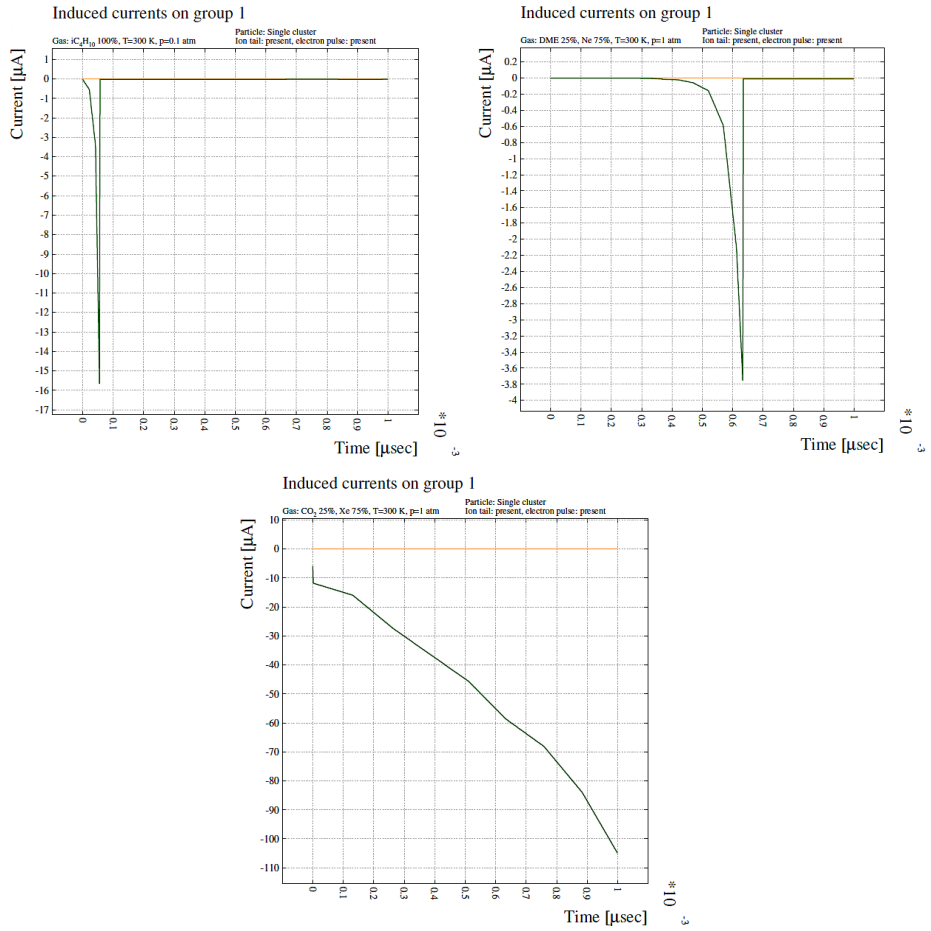

Figure 5.19: Signal obtained using geometry 2 by passing a 10KeV X-ray photon

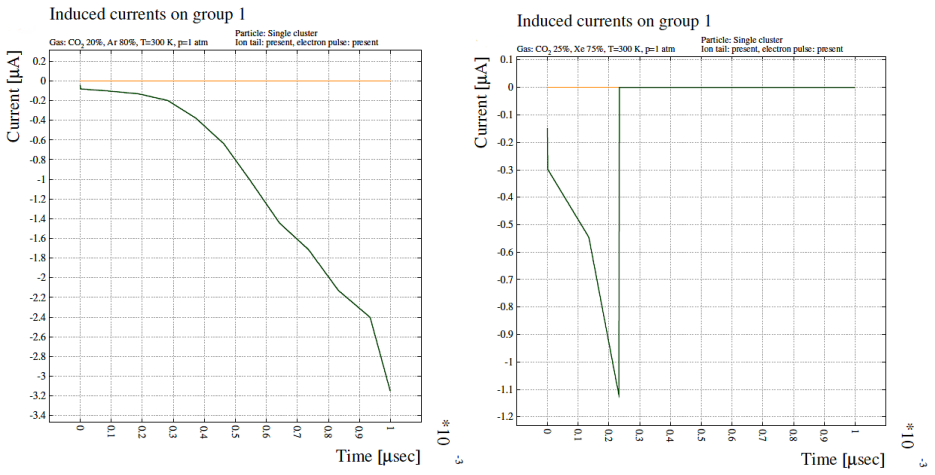

Figure 5.20: Signal obtained using geometry 2 by passing a 50KeV X-ray photon

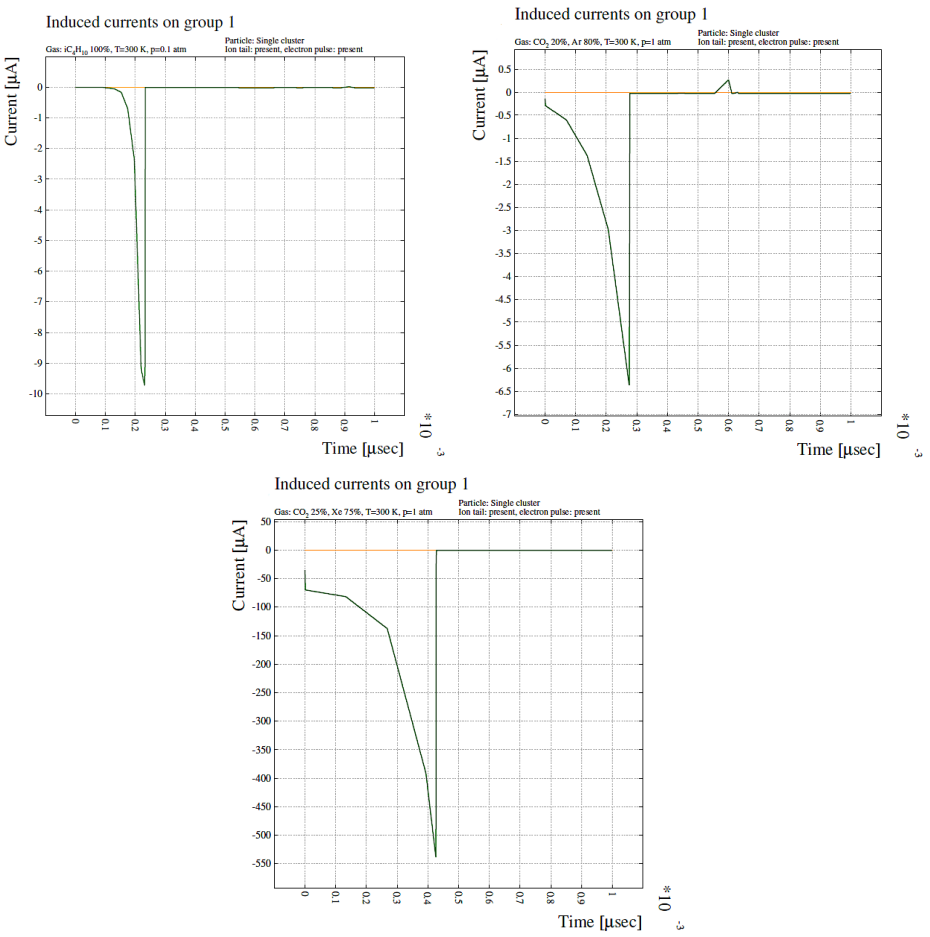

Figure 5.21: Signal obtained using geometry 2 by passing a 90KeV X-ray photon

Chapter 6

Simulations : Conclusion and Inferences

The simulation of the geometry as in section (5.4.1) shows two different geometry simulations. They are different on the basis of application of the amplification voltage whether it is applied on the read-out plane (Fig. 5.4) or on the micromesh (Fig. 5.5). The two types of chambers were simulated without any logical inconsistences. The simulations for the field configuration and drift lines have been shown in figures (5.6) to (5.9). Both the configurations are equally good in performance.
The Properties like electron drift velocity vs Electric field, the ionization and excitation rates etc (which are necessary for the gas medium simulation of the detector) of each gas used in the simulation, were calculated and plotted (for isobuatane (5.10), for the Ne:DME mixture (5.11), for the Ar:CO_2 mixture (5.12), for the $Xe : Co_2$ mixture (5.13)). These helps in the simulation of different processes that occur when the radiation interacts with the gas medium. The gas properties data is also necessary for the simulations of signal generation.

The signal obtained for the simulation of the passage of a

1. 1 KeV X-ray photon is shown as : for geometry 1 (Fig. 5.14) and for geometry 2 in (Fig. 5.18).

2. 10 KeV X-ray photon is shown as : for geometry 1 (Fig. 5.15) and for geometry 2 in (Fig. 5.19).

3. 50 KeV X-ray photon is shown as : (for geometry 1 (Fig. 5.16) and for geometry 2 in (Fig. 5.20).

4. 90 KeV X-ray photon is shown as : (for geometry 1 (Fig. 5.17 and for geometry 2 in (Fig. 5.21).

The tables below compile the signal data obtained.

Geometry 1				
X-ray photon energy / **Gas used**	1KeV	10 KeV	50 KeV	90 KeV
$Pure\ Isobutane$	0.73μA	11μA	0.8μA	N.O.
$Ne(80\%) : DME(20\%)$	8.0μA	1μA	0.2μA	0.2μA
$Ar(80\%) : Co_2(20\%)$	N.O.	80μA	3.3μA	N.O.
$Xe(80\%) : Co_2(20\%)$	280μA	N.O.	N.O.	N.O.

Table 6.1: Table showing the signal value obtained from the simulations for geometry 1

Geometry 2				
X-ray photon energy / **Gas used**	1KeV	10 KeV	50 KeV	90 KeV
$Pure\ Isobutane$	4.5μA	16μA	N.O.	10μA
$Ne(80\%) : DME(20\%)$	N.O.	3.8μA	N.O.	N.O.
$Ar(80\%) : Co_2(20\%)$	1.1μA	N.O.	3.2μA	6.5μA
$Xe(80\%) : Co_2(20\%)$	550μA	105μA	1.1μA	550μA

Table 6.2: Table showing the signal value obtained from the simulations for geometry 2

We can conclude that the detector responds to the X-ray photons of various energies, but the data misses few points, hence a more detailed study is needed. Further simulations and construction of a prototype can be carried to explore the further potential of the proposal of using micropattern gas detectors in X-ray astronomy.

Bibliography

[BAB+02] R. Bellazzini, F. Angelini, L. Baldini, A. Brez, E. Costa, L. Latronico, N. Lumb, M. M. Massai, N. Omodei, P. Soffitta, and G. Spandre, *X-ray polarimetry with a micro pattern gas detector with pixel readout*, IEEE Transactions on Nuclear Science **49 II** (2002), no. 3, 1216–1220.

[BAB+06] R. Bellazzini, F. Angelini, L. Baldini, F. Bitti, A. Brez, F. Cavalca, M. Del Prete, M. Kuss, L. Latronico, N. Omodei, M. Pinchera, M. M. Massai, M. Minuti, M. Razzano, C. Sgro, G. Spandre, A. Tenze, E. Costa, and P. Soffitta, *Gas pixel detectors for X-ray polarimetry applications*, Nuclear Instruments and Methods in Physics Research, Section A: Accelerators, Spectrometers, Detectors and Associated Equipment **560** (2006), no. 2, 425–434.

[BBB+03] R. Bellazzini, L. Baldini, A. Brez, E. Costa, L. Latronico, N. Omodei, P. Soffitta, and G. Spandre, *A photoelectric polarimeter based on a Micropattern Gas Detector for X-ray astronomy*, Nuclear Instruments and Methods in Physics Research, Section A: Accelerators, Spectrometers, Detectors and Associated Equipment, vol. 510, 2003, pp. 176–184.

[BBB+06] R. Bellazzini, L. Baldini, A. Brez, F. Cavalca, L. Latronico, N. Omodei, M.M. Massai, M. Minuti, M. Razzano, C. Sgro, G. Spandre, E. Costa, and P. Soffitta, *Gas pixel detectors for high-sensitivity X-ray polarimetry*, Proceedings of SPIE - The International Society for Optical Engineering, vol. 6266 II, 2006.

[BBC+13] Ronaldo Bellazzini, Alessandro Brez, Enrico Costa, Massimo Minuti, Fabio Muleri, Michele Pinchera, Alda Rubini, Paolo Soffitta, and Gloria Spandre, *Photoelectric X-ray polarimetry with gas pixel detectors*, Nuclear Instruments

and Methods in Physics Research, Section A: Accelerators, Spectrometers, Detectors and Associated Equipment **720** (2013), 173–177.

[Bia] Stephen Biagi, *Magboltz - transport of electrons in gas mixtures*, $http$: $//magboltz.web.cern.ch/magboltz/$.

[BM10] R. Bellazzini and F. Muleri, *X-ray polarimetry: A new window on the high energy sky*, Nuclear Instruments and Methods in Physics Research, Section A: Accelerators, Spectrometers, Detectors and Associated Equipment **623** (2010), no. 2, 766–770.

[DTF03] A. Das Thomas Ferbel, *Introduction to nuclear and particle physics*, World Scientific, 2003.

[gem] *Gas electron multiplier*, $https://en.wikipedia.org/wiki/Gas\_electron\_multiplier$.

[goo] *Google image search*, $images.google.com$.

[Kno89] G.F. Knoll, *Radiation detection and measurement*, Wiley, 1989.

[Leo87] W.R. Leo, *Techniques for nuclear and particle physics experiments: a how-to approach*, Springer-Verlag, 1987.

[mic] *Micromegas detector*, $https://en.wikipedia.org/wiki/MicroMegas\_detector$.

[rad] *Radiation*, $https://en.wikipedia.org/wiki/Radiation$.

[SM] Nayana Majumdar Supratik Mukhopadhay, *A nearly exact boundary element method*, $http://nebem.web.cern.ch/nebem/$.

[Smi] Igor Smirnov, *Heed: Interactions of particles with gases*, $https://lost-contact.mit.edu/afs/cern.ch/project/writeups/Abstracts/heed.html$,$https://heed.web.cern.ch/heed/$.

[Sra] *Shockley–ramo theorem*, https://en.wikipedia.org/wiki/Shockley%E2%80%93Ramo_theorem.

[STY10] T. Sato, T. Takahashi, and K. Yoshimura, *Particle and nuclear physics at j-parc*, Lecture Notes in Physics, Springer Berlin Heidelberg, 2010.

[Vee] Rob Veenhof, *Garfield - simulation of gaseous detectors*, $http://garfield.web.cern.ch/garfield/$.

[wika] *X-ray*, $https://en.wikipedia.org/wiki/X-ray$.

[wikb] *X-ray astronomy*, $https://en.wikipedia.org/wiki/X-ray\_astronomy$.